

# ALTIUS In-flight Calibration Activities

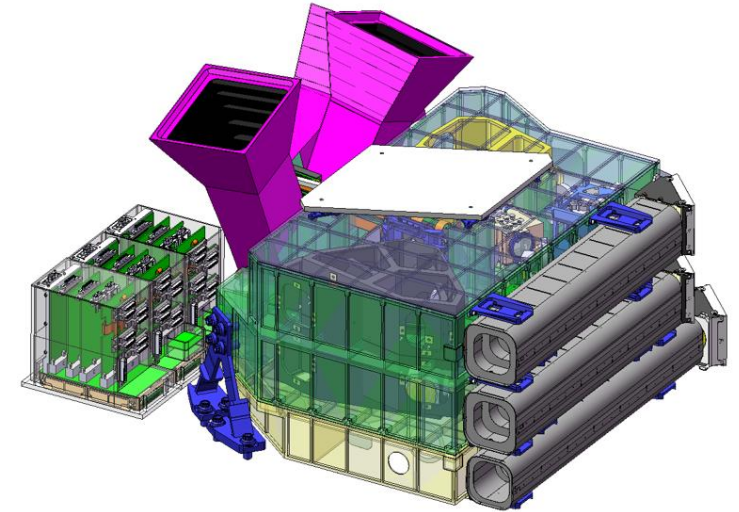
**Authors:**

N. Lloyd <sup>1</sup>, K. Jensen <sup>1</sup>, D. Degenstein <sup>1</sup>,  
J. Naudet <sup>2</sup>, A. Famelaer <sup>2</sup>.

<sup>1</sup> University of Saskatchewan, Canada

<sup>2</sup> Redwire, Belgium.

**ATMOS, 1 July 2024, Bologna.**



# ALTIUS In-flight Calibration Activities

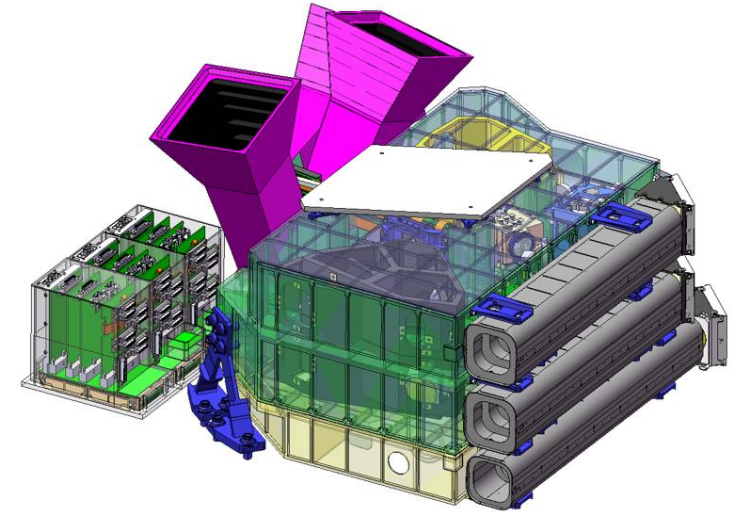
**Authors:**

N. Lloyd <sup>1</sup>, K. Jensen <sup>1</sup>, D. Degenstein <sup>1</sup>,  
J. Naudet <sup>2</sup>, A. Famelaer <sup>2</sup>.

<sup>1</sup> University of Saskatchewan, Canada

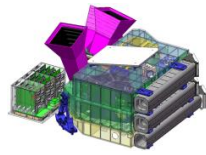
<sup>2</sup> Redwire, Belgium.

**ATMOS, 1 July 2024, Bologna.**

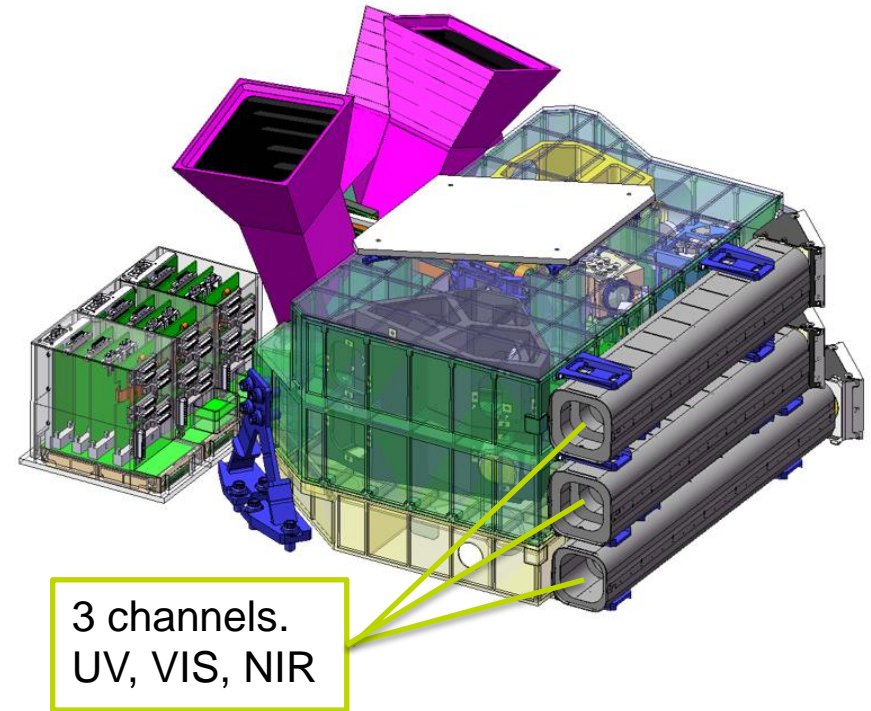


A quick guided tour. Sit back and enjoy.

# Optical Description

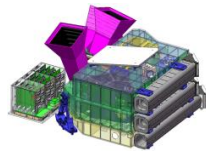


ALTIUS is a spectral imaging system. It can collect signal on 3 optical channels.



3 channels.  
UV, VIS, NIR

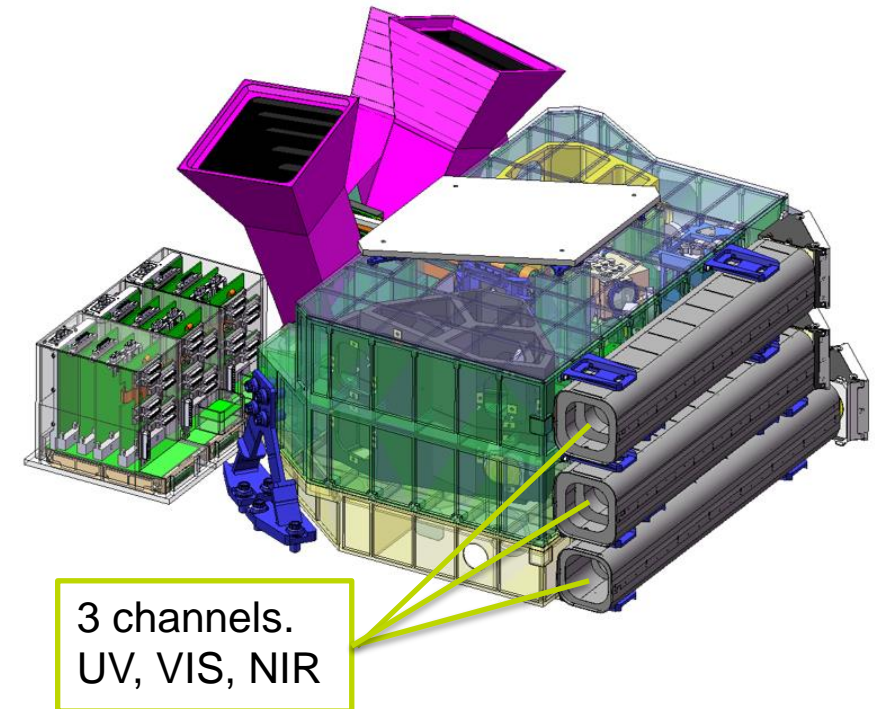
# Optical Description



ALTIUS is a spectral imaging system. It can collect signal on 3 optical channels.

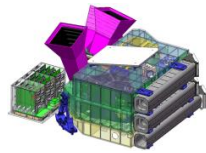
There are 7 optical configurations:

Channel	Wavelength Range	Filter Technology	Bright Limb	Solar Occultation	Stellar Occultation
UV	250 – 355 nm	Stacked FPI	✓	✓	✓
VIS	440 – 675 nm	AOTF	✓	✓	
NIR	600 – 1020 nm	AOTF	✓	✓	



3 channels.  
UV, VIS, NIR

# Optical Description



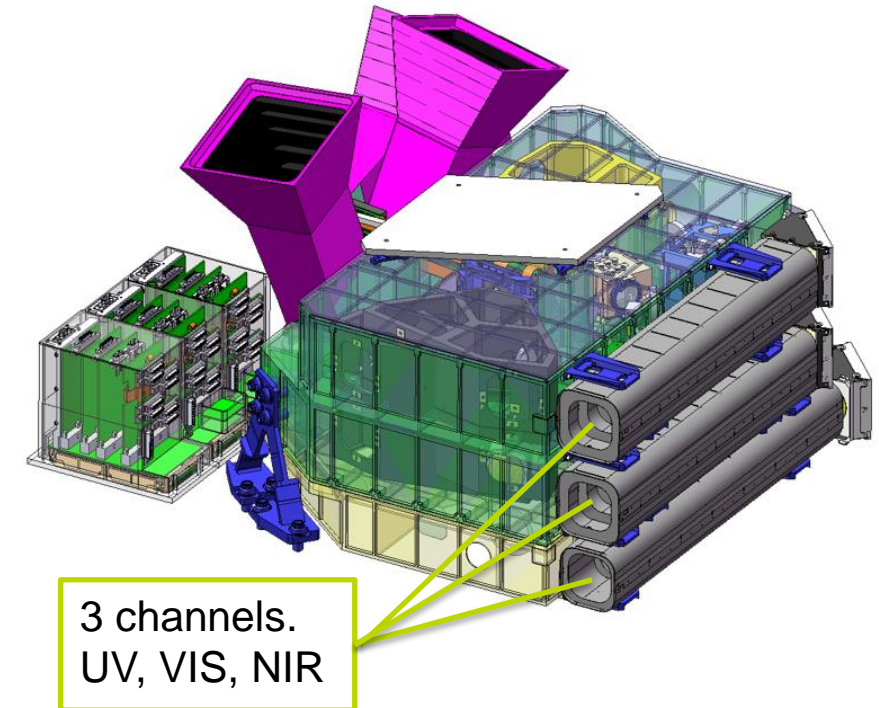
ALTIUS is a spectral imaging system. It can collect signal on 3 optical channels.

There are 7 optical configurations:

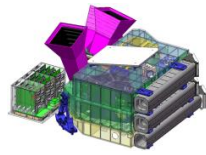
Channel	Wavelength Range	Filter Technology	Bright Limb	Solar Occultation	Stellar Occultation
UV	250 – 355 nm	Stacked FPI	✓	✓	✓
VIS	440 – 675 nm	AOTF	✓	✓	
NIR	600 – 1020 nm	AOTF	✓	✓	

Each channel has a  $2^\circ \times 2^\circ$  FOV

Channel	Field of View	Front End Optics	Detector	Raw Image Size	Science Size (binning = 3)
UV	$2^\circ \times 2^\circ$ $0.36^\circ \times 0.36^\circ$	Telescopic	Teledyne CIS315	513 x 513	171 x 171
VIS	$2^\circ \times 2^\circ$	Telecentric	Teledyne CIS315	1503 x 1503	501 x 501
NIR	$2^\circ \times 2^\circ$	Telecentric	Teledyne CIS315	1503 x 1503	501 x 501

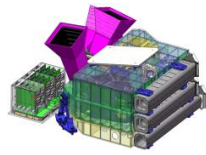


# ALTIUS In-flight calibration:



ALTIUS has no onboard calibration equipment. All inflight calibration must be performed using natural sources.

# ALTIUS In-flight calibration:

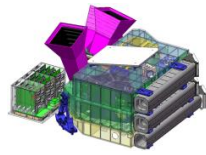


ALTIUS has no onboard calibration equipment. All inflight calibration must be performed using natural sources.

Calibrations discussed in this presentation.

Calibration	Technique
PRNU	Raster Scan of the Solar disk.
PSF Core	Lunar disk as a circular edge for PSF/MTF.
PSF Tails	Lunar disk located just outside the field of view.
Wavelength Registration	Solar disk: Fraunhofer lines.
Polarization	Rayleigh scattering off Earth's upper atmosphere.

# ALTIUS In-flight calibration:



ALTIUS has no onboard calibration equipment. All inflight calibration must be performed using natural sources.

Calibrations discussed in this presentation.

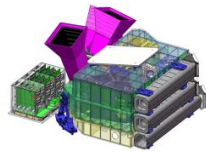
Calibration	Technique
PRNU	Raster Scan of Solar disk.
PSF Core	Lunar disk as circular edge for PSF/MTF.
PSF Tails	Lunar disk located just outside the field of view.
Wavelength Registration	Solar disk: Fraunhofer lines.
Polarization	Rayleigh scattering off Earth's upper atmosphere.

Other calibrations not discussed here.

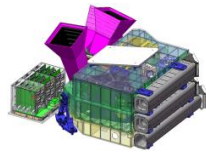
Calibration	Technique
Abs-cal	SAO2010 Solar irradiance applied to observations of the solar disk.
Abs-cal	ROLO/Lime/Llamas applied to Lunar Irradiance in bright limb configuration.
Abs-cal	Observation of calibrated bright star (e.g. Vega/Sirius). Stellar occultation configuration. UV channel only.
SRF	No available natural targets. E.g. Auroral lines are not sufficiently temporally stable or predictable.



# PRNU: Strategy

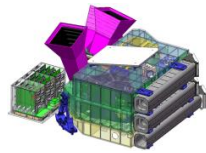


Standard PRNU calibration requires illuminating the aperture with a uniform source. ALTIUS must choose a natural source. There are many possibilities, for example:



Standard PRNU calibration requires illuminating the aperture with a uniform source. ALTIUS must choose a natural source. There are many possibilities, for example:

- Solar disk. Smooth but very bright/hot. Possible operational issues.
- Lunar disk. A lot of spatial features that must be accurately modelled if used as a PRNU calibration. Very difficult.
- Cloud tops. Always structure of some sort. Poor signal at the UV wavelengths. Difficult to predict in advance.
- Libyan Desert. Always time dependent structure. No signal at UV wavelengths. Difficult to predict cloud free conditions in advance.
- Antarctica/Dome-C/Greenland. Always time dependent structure. No signal at UV wavelengths. Difficult to predict cloud free conditions in advance.



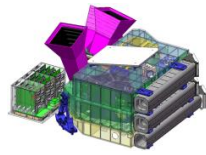
Standard PRNU calibration requires illuminating the aperture with a uniform source. ALTIUS must choose a natural source. There are many possibilities, for example:

- Solar disk. Smooth but very bright/hot. Possible operational issues.
- Lunar disk. A lot of spatial features that must be accurately modelled if used as a PRNU calibration. Very difficult.
- Cloud tops. Always structure of some sort. Poor signal at the UV wavelengths. Difficult to predict in advance.
- Libyan Desert. Always time dependent structure. No signal at UV wavelengths. Difficult to predict cloud free conditions in advance.
- Antarctica/Dome-C/Greenland. Always time dependent structure. No signal at UV wavelengths. Difficult to predict cloud free conditions in advance.

## Our strategy:

1. Use observations of the Solar disk with neutral density filter to calibrate the Solar Occultation configuration.
2. Assume we can model small vignetting terms due to the neutral density filter. Then we can calculate the PRNU for the Bright Limb and Stellar Occultation configurations directly from the Solar Disk calibrations.

# PRNU: Solar Disk Concept



- Sun is too small to fill the field of view,  $0.5^\circ$  versus  $2.0^\circ$  so we must raster scan the Sun across the field of view.
- Sun is not uniform, and we must apply a limb darkening correction to flatten the images.
- Generate the PRNU from a weighted average of the raster scan images

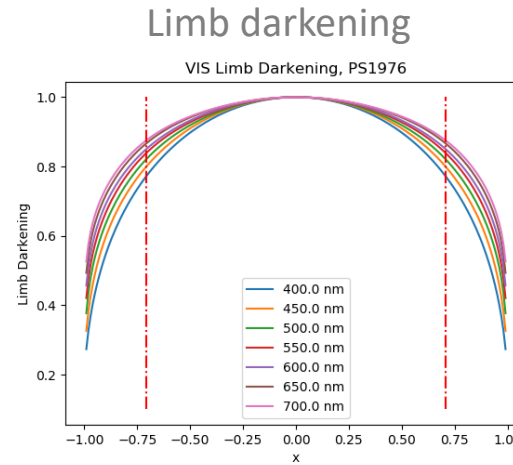
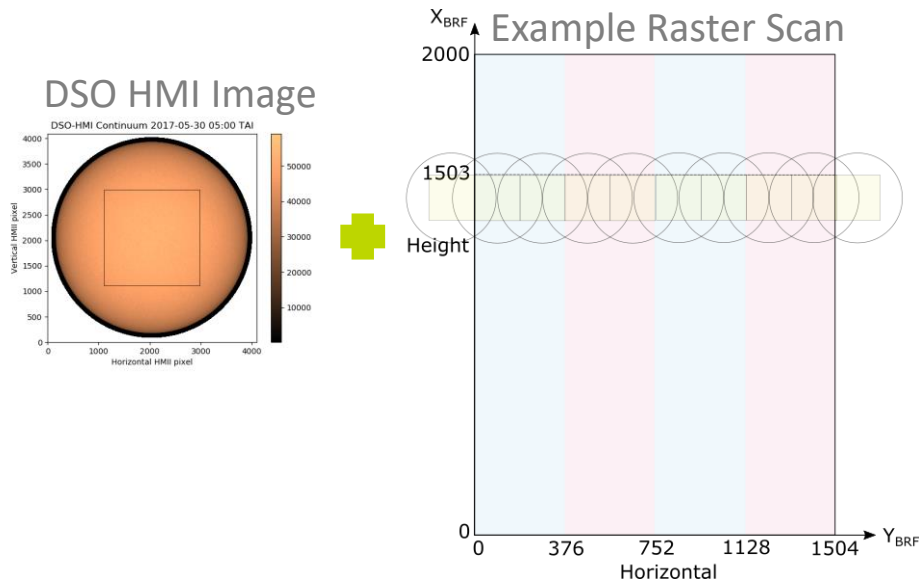
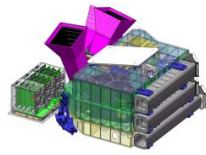


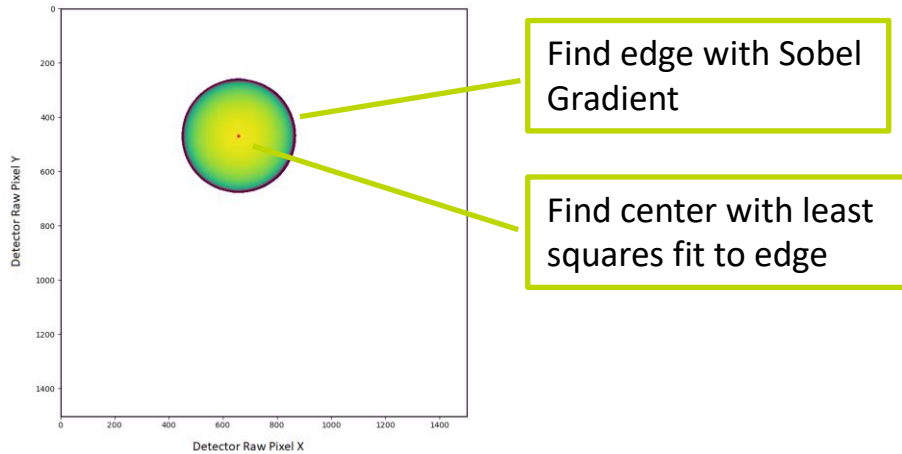
Table of solar images covering the field of view

99	98	97	96	95	94	93	92	91	90
80	81	82	83	84	85	86	87	88	89
79	78	77	76	75	74	73	72	71	70
60	61	62	63	64	65	66	67	68	69
59	58	57	56	55	54	53	52	51	50
40	41	42	43	44	45	46	47	48	49
39	38	37	36	35	34	33	32	31	30
20	21	22	23	24	25	26	27	28	29
19	18	17	16	15	14	13	12	11	10
0	1	2	3	4	5	6	7	8	9

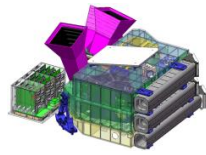


## 1. Center Determination

1. Determine the center of each image of the Sun.
2. Find the edge using a Sobel gradient operator.
3. Fit a circle to the edge locations.

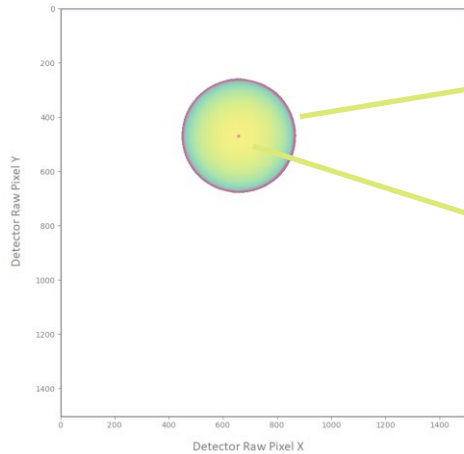


# PRNU: Image Flattening



## 1. Center Determination

1. Determine the center of each image of the Sun.
2. Find the edge using a Sobel gradient operator.
3. Fit a circle to the edge locations.



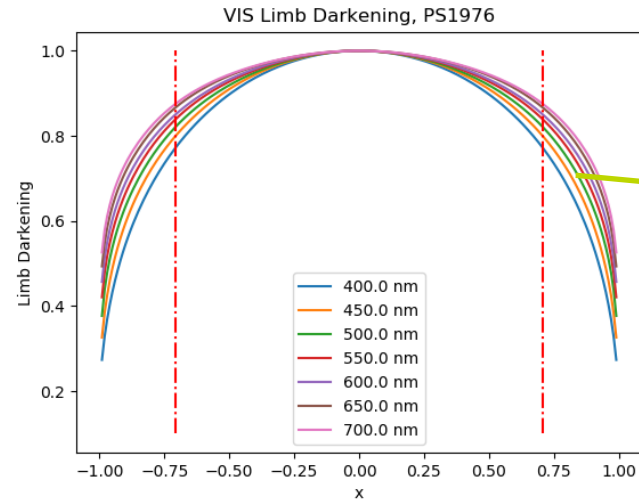
Find edge with Sobel Gradient

Find center with least squares fit to edge



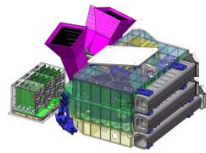
## 2. Limb Darkening

1. Limb darkening is a function of angle from the center of the Sun.
2. Use the limb darkening curves of Pierce and Slaughter (or similar).
3. We must measure our own curves between 250 nm and 320 nm.
4. Heavily weight/ignore points located too far from the center.



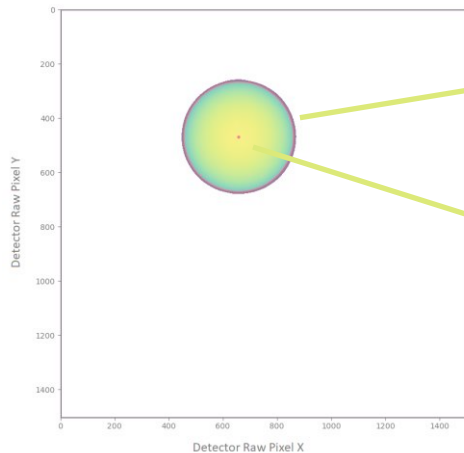
Discard regions near the solar limb using weights

# PRNU: Image Flattening



## 1. Center Determination

1. Determine the center of each image of the Sun.
2. Find the edge using a Sobel gradient operator.
3. Fit a circle to the edge locations.



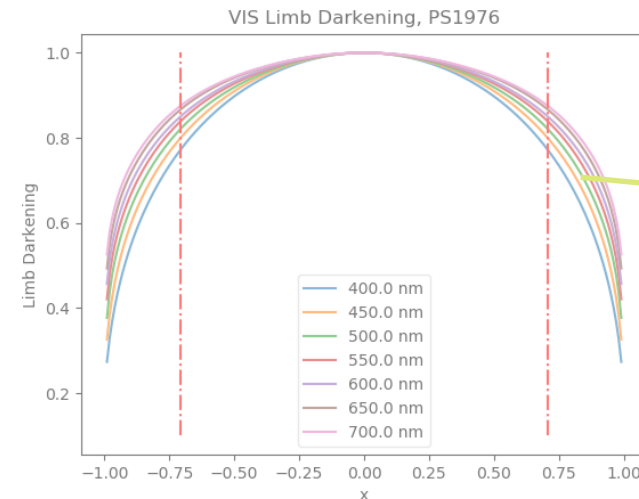
Find edge with Sobel Gradient

Find center with least squares fit to edge



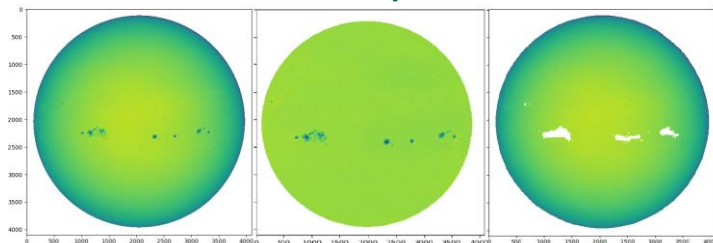
## 2. Limb Darkening

1. Limb darkening is a function of angle from the center of the Sun.
2. Use the limb darkening curves of Pierce and Slaughter (or similar).
3. We must measure our own curves between 250 nm and 320 nm.
4. Heavily weight/ignore points located too far from the center.



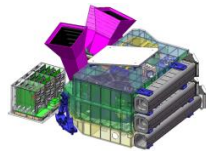
Discard regions near the solar limb using weights

## 3. Mask out sunspots



1. Flatten the solar disk using limb darkening.
2. Detect sunspots using thresholding
3. Mask out sunspots so they have zero weight.

# PRNU: Stitching



The PRNU calibration generates approximately 100 separate images at each wavelength setting. These images must be stitched together to make a single map. This is done using the weight map .

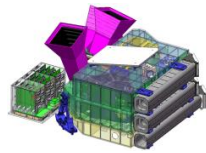
1. Each solar disk image provides an estimate of PRNU for a limited selection of pixels on the detector area.
2. Each estimate is assigned a weight base upon the data quality, central regions receive higher weight.
3. The PRNU is taken from the weighted average of all contributions to each pixel.

Measured Solar Disk Table

99	98	97	96	95	94	93	92	91	90
80	81	82	83	84	85	86	87	88	89
79	78	77	76	75	74	73	72	71	70
60	61	62	63	64	65	66	67	68	69
59	58	57	56	55	54	53	52	51	50
40	41	42	43	44	45	46	47	48	49
39	38	37	36	35	34	33	32	31	30
20	21	22	23	24	25	26	27	28	29
19	18	17	16	15	14	13	12	11	10
0	1	2	3	4	5	6	7	8	9



# PRNU: Stitching



The PRNU calibration generates approximately 100 separate images at each wavelength setting. These images must be stitched together to make a single map. This is done using the weight map .

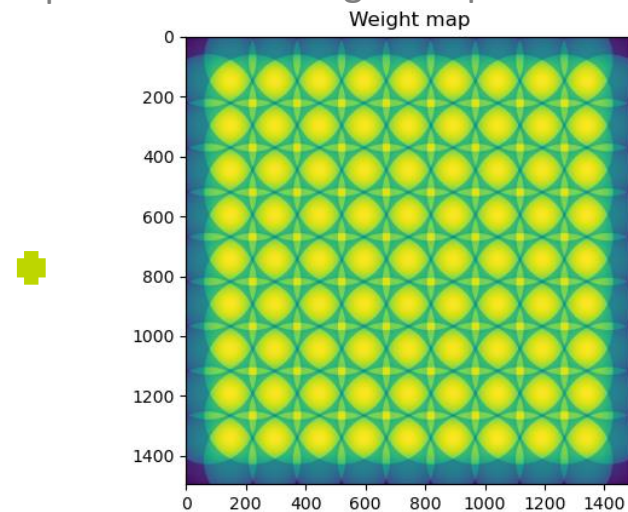
1. Each solar disk image provides an estimate of PRNU for a limited selection of pixels on the detector area.
2. Each estimate is assigned a weight base upon the data quality, central regions receive higher weight.
3. The PRNU is taken from the weighted average of all contributions to each pixel.

Measured Solar Disk Table

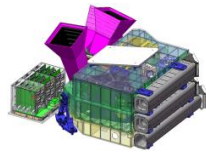
99	98	97	96	95	94	93	92	91	90
80	81	82	83	84	85	86	87	88	89
79	78	77	76	75	74	73	72	71	70
60	61	62	63	64	65	66	67	68	69
59	58	57	56	55	54	53	52	51	50
40	41	42	43	44	45	46	47	48	49
39	38	37	36	35	34	33	32	31	30
20	21	22	23	24	25	26	27	28	29
19	18	17	16	15	14	13	12	11	10
0	1	2	3	4	5	6	7	8	9

plus

Weight Map



# PRNU: Stitching



The PRNU calibration generates approximately 100 separate images at each wavelength setting. These images must be stitched together to make a single map. This is done using the weight map .

1. Each solar disk image provides an estimate of PRNU for a limited selection of pixels on the detector area.
2. Each estimate is assigned a weight base upon the data quality, central regions receive higher weight.
3. The PRNU is taken from the weighted average of all contributions to each pixel.

Measured Solar Disk Table

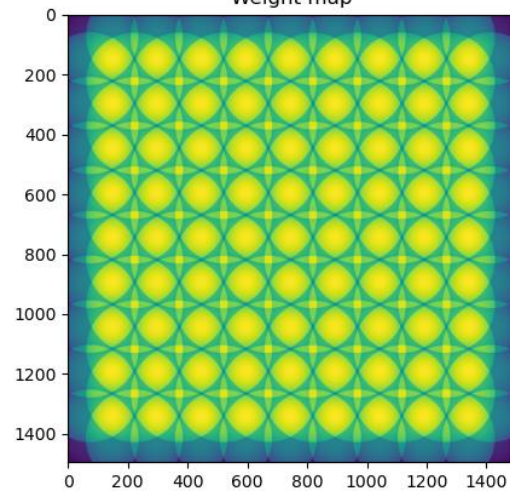
99	98	97	96	95	94	93	92	91	90
80	81	82	83	84	85	86	87	88	89
79	78	77	76	75	74	73	72	71	70
60	61	62	63	64	65	66	67	68	69
59	58	57	56	55	54	53	52	51	50
40	41	42	43	44	45	46	47	48	49
39	38	37	36	35	34	33	32	31	30
20	21	22	23	24	25	26	27	28	29
19	18	17	16	15	14	13	12	11	10
0	1	2	3	4	5	6	7	8	9

plus



Weight Map

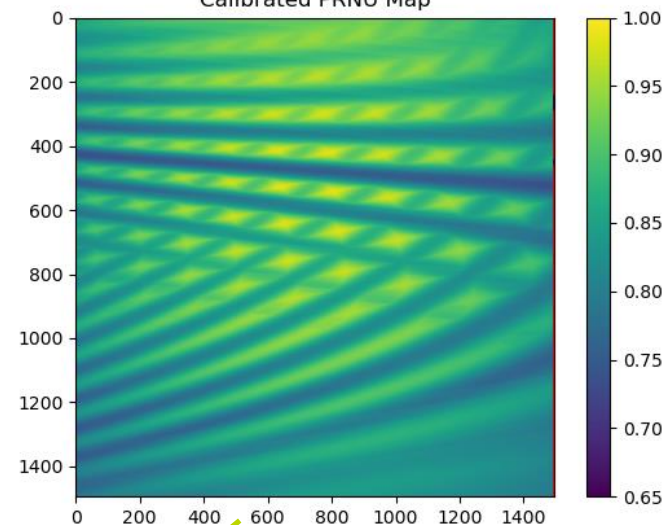
Weight map



makes

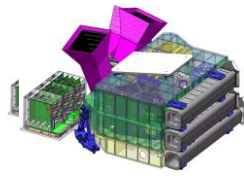
PRNU Map

Calibrated PRNU Map



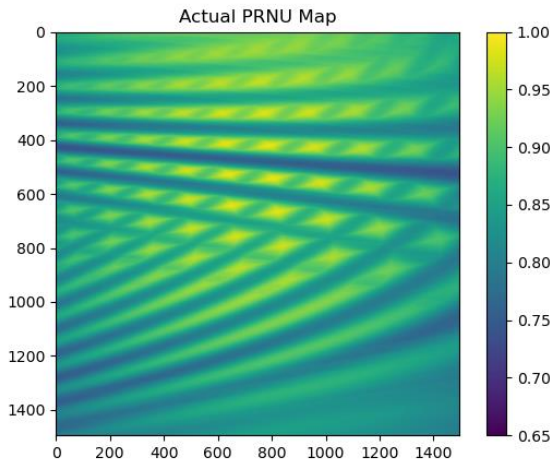
The VIS/NIR channels have a lot of spatial structure due to telecentric optics imaging near to the AOTF.

# PRNU: Results

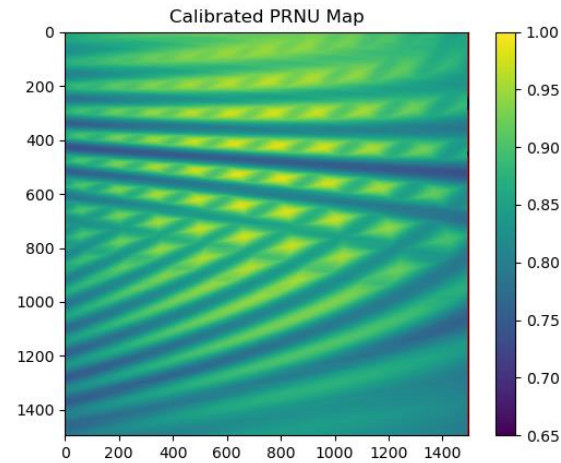


We simulated the solar PRNU calibration using a PRNU provided by the instrument builder. We can achieve a PRNU with a stochastic error around 0.6%.

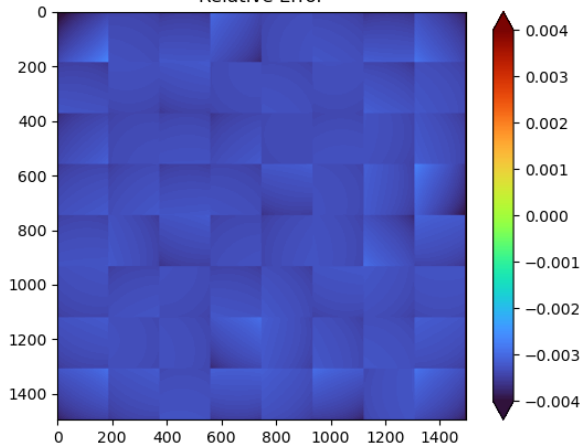
Original PRNU



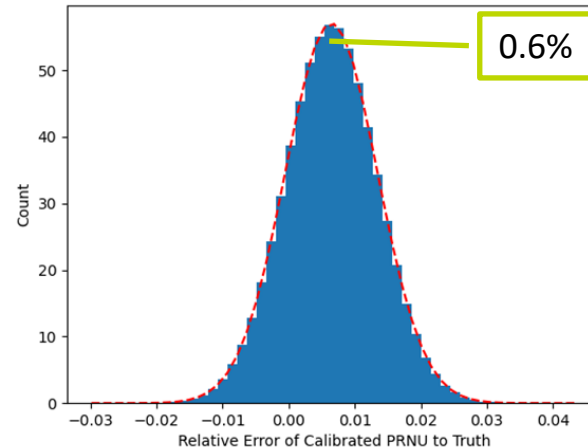
Retrieved PRNU



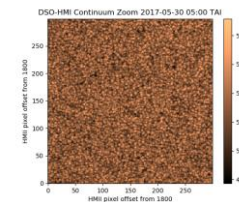
Relative Error

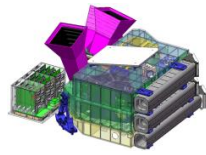


Calibration Relative Error for 600.0 nm PRNU  
 $\mu = 0.006, \sigma = 0.007$



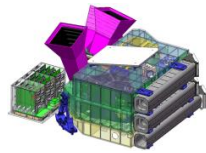
1. The VIS/NIR PRNU has a lot of spatial structure due to the telecentric optics: each pixel only uses a small part of the AOTF crystal area.
2. Primary systematic error is center determination. This creates a systematic error in the limb darkening correction.
3. Solar granulation is ignored. The granulation size is about 1/3 the size of a raw pixel or 1/9<sup>th</sup> the size of a binned science pixel.





The point spread function has two primary domains,

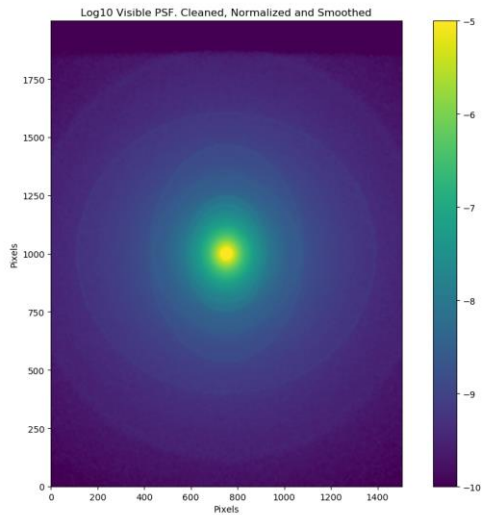
1. A central core region controlled by standard optical aberrations.
2. An extended tail region controlled by scattering off various surface imperfections.

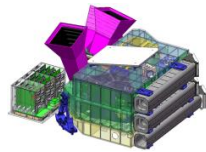


The point spread function has two primary domains,

1. A central core region controlled by standard optical aberrations.
2. An extended tail region controlled by scattering off various surface imperfections.

PSF supplied by instrument  
builder for VIS channel.

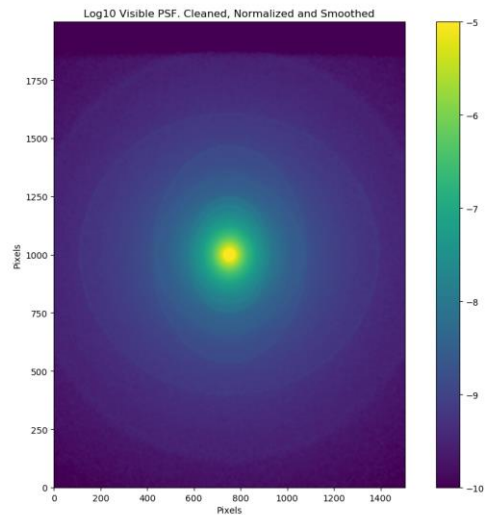




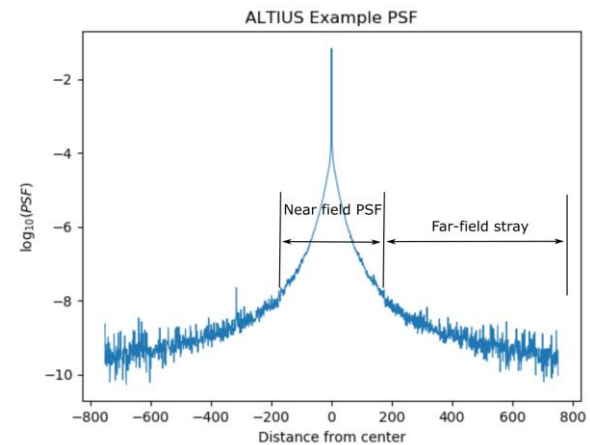
The point spread function has two primary domains,

1. A central core region controlled by standard optical aberrations.
2. An extended tail region controlled by scattering off various surface imperfections.

PSF supplied by instrument builder for VIS channel.



Characterized by sharp central region: PSF Core, and slowly varying outer Region: PSF tails

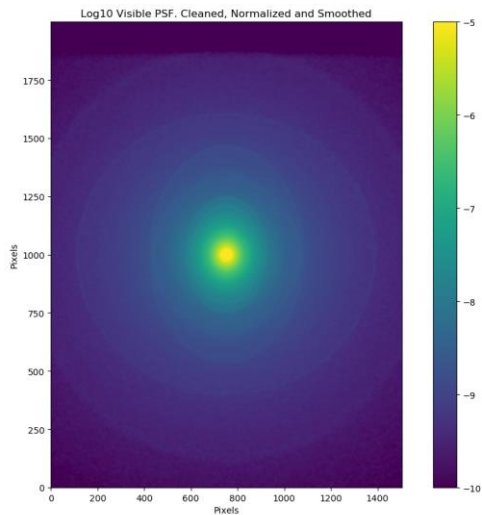




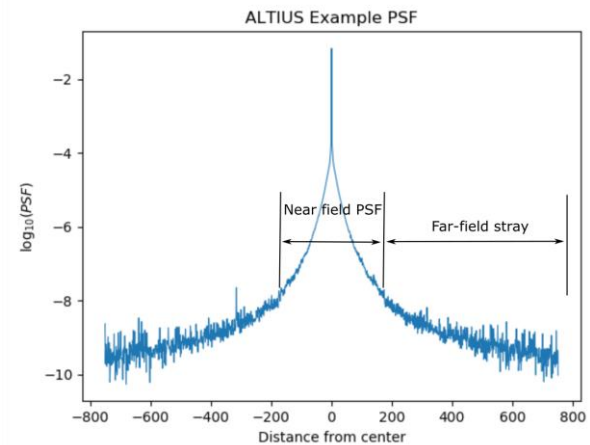
The point spread function has two primary domains,

1. A central core region controlled by standard optical aberrations.
2. An extended tail region controlled by scattering off various surface imperfections.

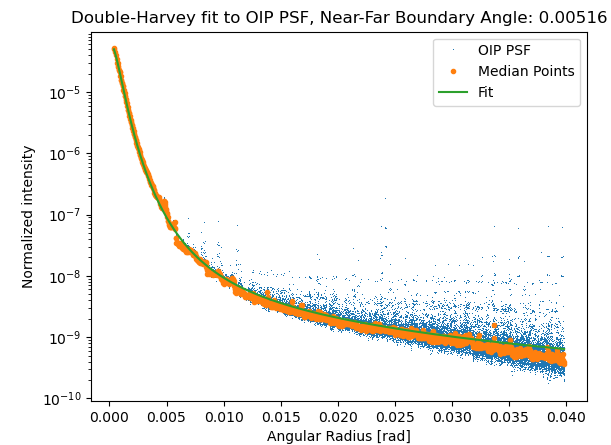
PSF supplied by instrument builder for VIS channel.



Characterized by sharp central region: PSF Core, and slowly varying outer Region: PSF tails

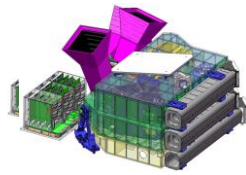


PSF tail region can be approximated by fitting two Harvey curves.



$$P(\Theta) = B_{0,near} \left[ 1 + \left( \frac{\Theta}{l_{near}} \right)^2 \right]^{-\frac{S_{near}}{2}} + B_{0,far} \left[ 1 + \left( \frac{\Theta}{l_{far}} \right)^2 \right]^{-\frac{S_{far}}{2}}$$

# PSF: Calibration Strategy

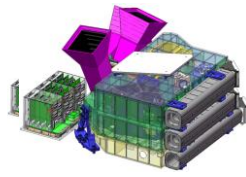


Several possibilities for the PSF Core exist.

- Craters on the lunar surface (e. g. Bessel crater in the Sea of Serenity).
- Stars. Too dim and require very stable pointing requirements.
- Straight edges of glaciers or bridges using MTF straight-edge techniques.
- Curved edge of Moon using modified MTF straight-edge techniques.



# PSF: Calibration Strategy



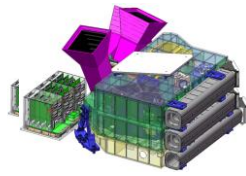
Several possibilities for the PSF Core exist.

- Craters on the lunar surface (e. g. Bessel crater in the Sea of Serenity).
- Stars. Too dim and require very stable pointing requirements.
- Straight edges of glaciers or bridges using MTF straight-edge techniques.
- Curved edge of Moon using modified MTF straight-edge techniques.

Several possibilities for the PSF Tails exist.

- Bright object (Moon or Sun) just outside the field of view.
- Bright object (Moon or Sun) inside the field of view. Blooming effects may be a concern.
- Vertical scan of bright Earth limb.

# PSF: Calibration Strategy



Several possibilities for the PSF Core exist.

- Craters on the lunar surface (e. g. Bessel crater in the Sea of Serenity).
- Stars. Too dim and require very stable pointing requirements.
- Straight edges of glaciers or bridges using MTF straight-edge techniques.
- Curved edge of Moon using modified MTF straight-edge techniques.

Several possibilities for the PSF Tails exist.

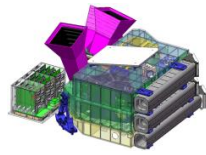
- Bright object (Moon or Sun) just outside the field of view.
- Bright object (Moon or Sun) inside the field of view. Blooming effects may be a concern.
- Vertical scan of bright Earth limb.

## Our strategy:

Use the Moon to calibrate both the PSF Tails and the PSF Core.

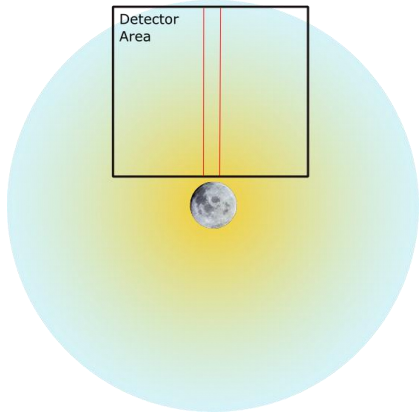
1. Measure the PSF Tails using the moon just outside the field of view.
2. Measure the PSF Core using the curved edge of the lunar disk.

# PSF Tails using the Moon

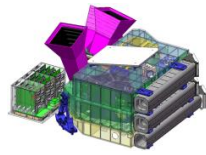


Place the Moon just outside the field of view and look at the weak scattered signal on the detector.

1. Place moon near an edge of the FOV. And move it around.

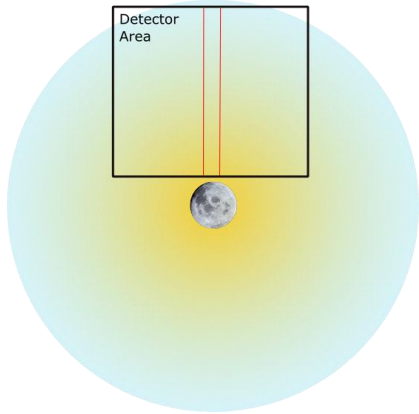


# PSF Tails using the Moon

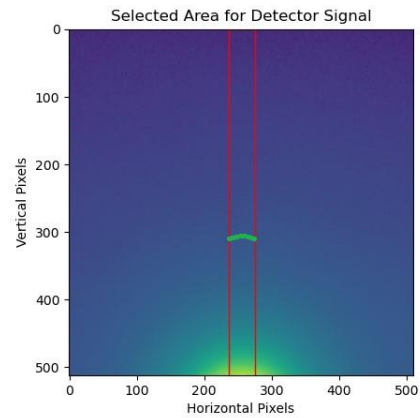


Place the Moon just outside the field of view and look at the weak scattered signal on the detector.

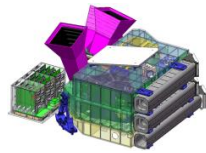
1. Place moon near an edge of the FOV. And move it around.



2. For each Moon position, restrict signal to small strip.

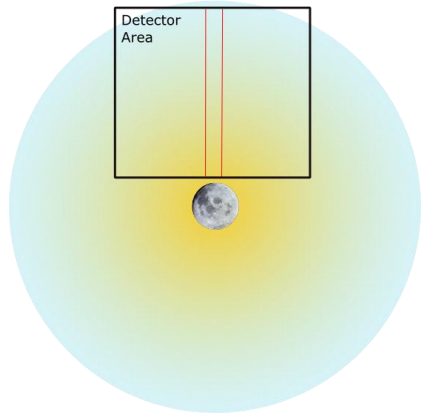


# PSF Tails using the Moon

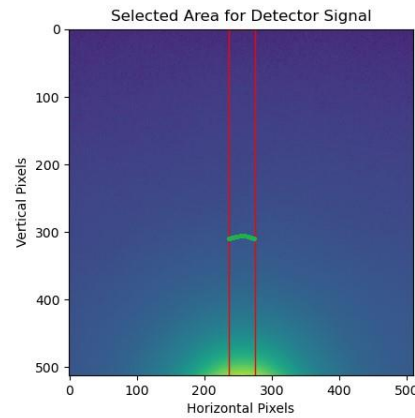


Place the Moon just outside the field of view and look at the weak scattered signal on the detector.

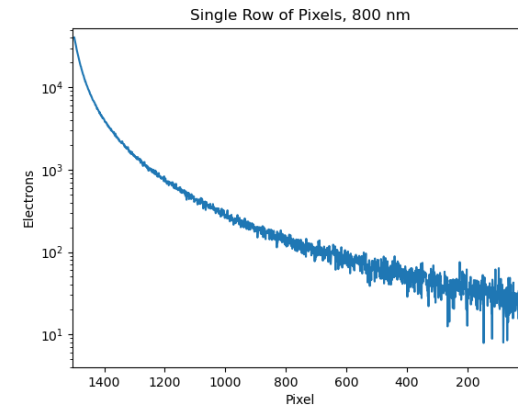
1. Place moon near an edge of the FOV. And move it around.



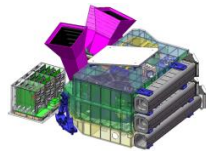
2. For each Moon position, restrict signal to small strip.



3. Integrate measured signal along strip.

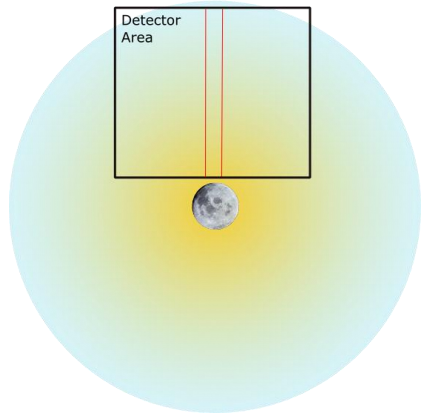


# PSF Tails using the Moon

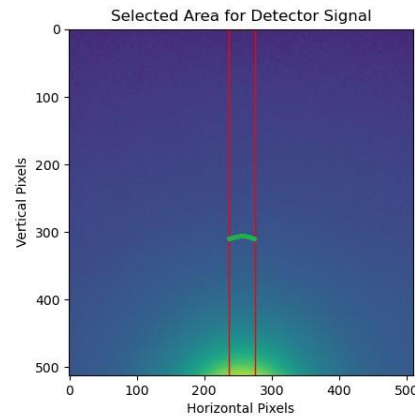


Place the Moon just outside the field of view and look at the weak scattered signal on the detector.

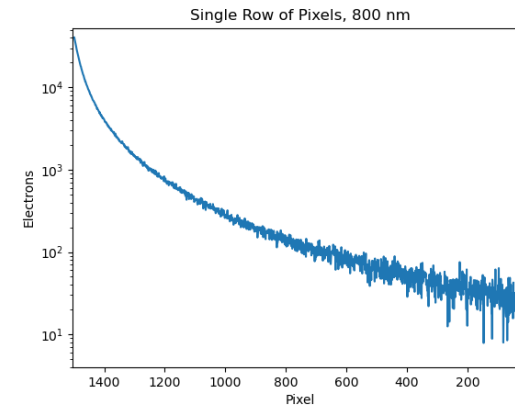
1. Place moon near an edge of the FOV. And move it around.



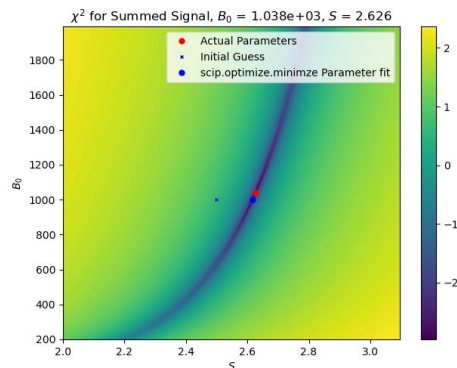
2. For each Moon position, restrict signal to small strip.



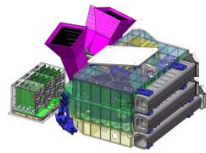
3. Integrate measured signal along strip.



4. LSQ double Harvey curve.  $\chi^2$  has a long valley. Need to be careful .

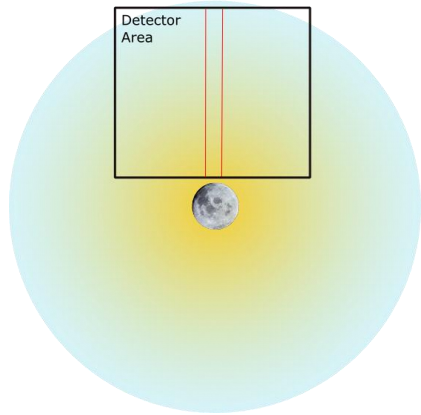


# PSF Tails using the Moon

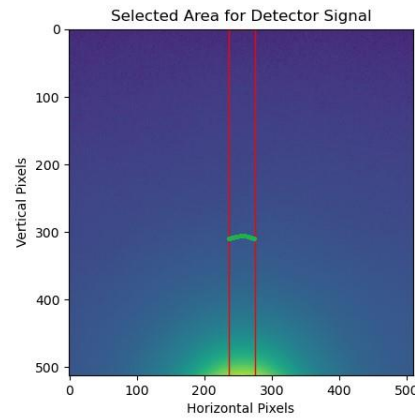


Place the Moon just outside the field of view and look at the weak scattered signal on the detector.

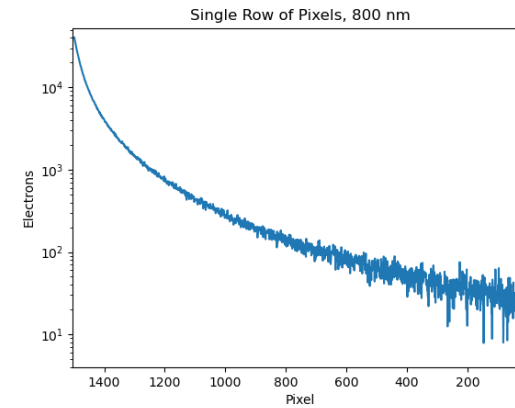
1. Place moon near an edge of the FOV. And move it around.



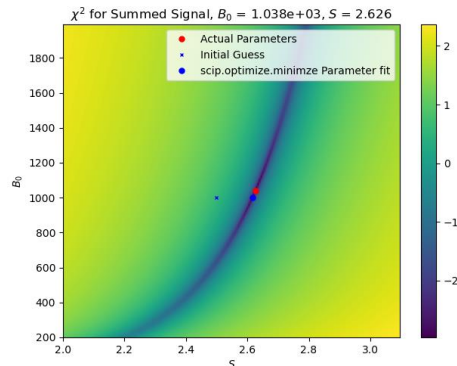
2. For each Moon position, restrict signal to small strip.



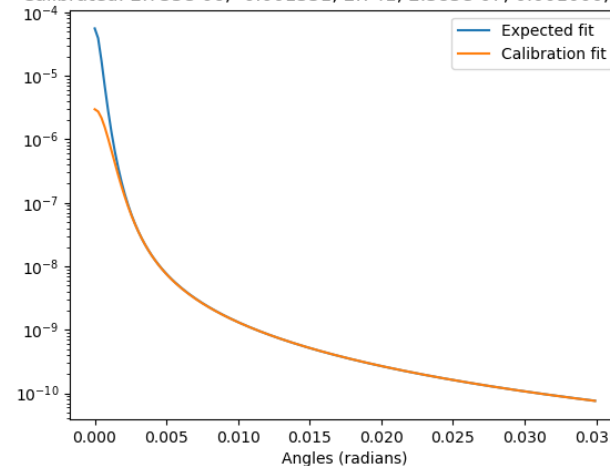
3. Integrate measured signal along strip.



4. LSQ double Harvey curve.  $\chi^2$  has a long valley. Need to be careful.

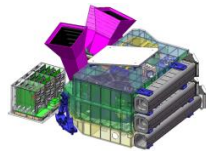


Comparison of Close Source fit and actual PSF, az: 0.022, el: 0.000  
 Expected: 5.541e-05, 0.000589, 2.402, 2.259e-07, 0.001000, 1.125  
 Calibrated: 2.733e-06, -0.001331, 2.741, 2.383e-07, 0.001000, 1.132



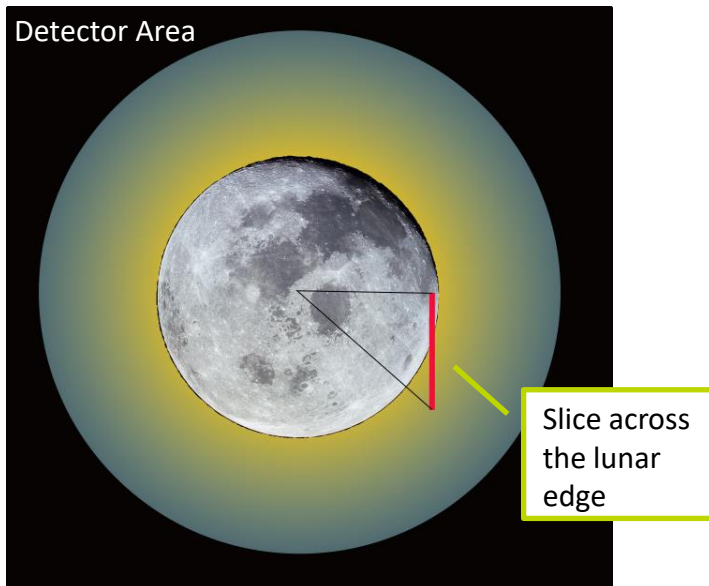
5. Resultant PSF Tail fit is good except at short radii close to the edge of the detector area.

# PSF Core using the Moon



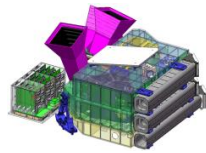
PSF Core calibration based upon adjusting the standard straight edge technique (ISO 12233 ) to the curved edge of the lunar disk. Others have tried this before: [Caron and Rollins, 2020](#).

1. Image moon on detector.  
Select various slices around the edge of the moon





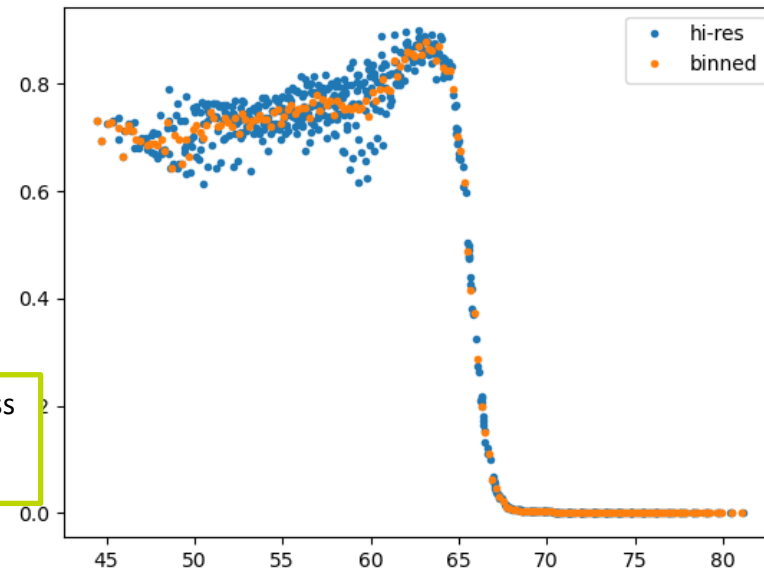
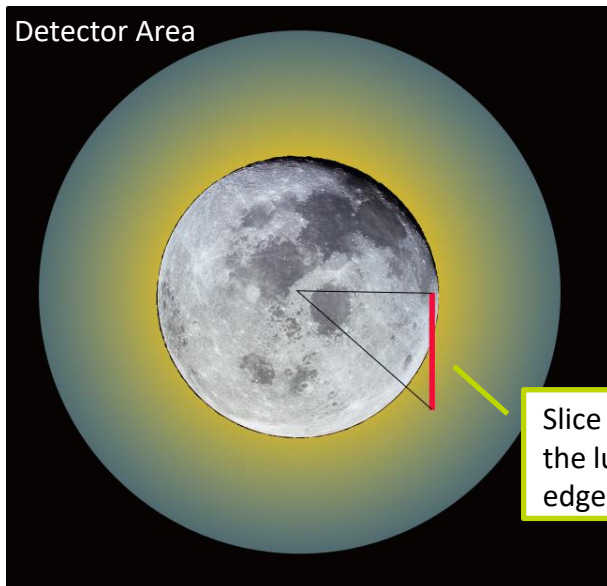
# PSF Core using the Moon



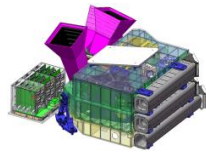
PSF Core calibration based upon adjusting the standard straight edge technique (ISO 12233 ) to the curved edge of the lunar disk. Others have tried this before: [Caron and Rollins, 2020](#).

1. Image moon on detector.  
Select various slices around the edge of the moon

2. For each slice generate an Edge Spread Function (ESF) as a function of radius. This allows super-sampling.

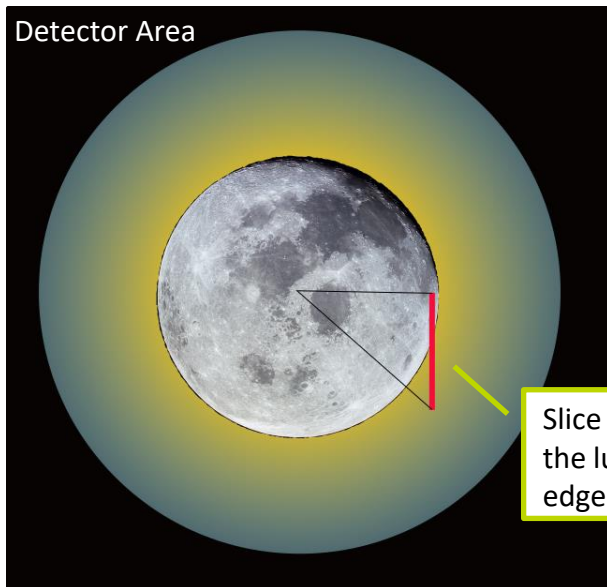


# PSF Core using the Moon

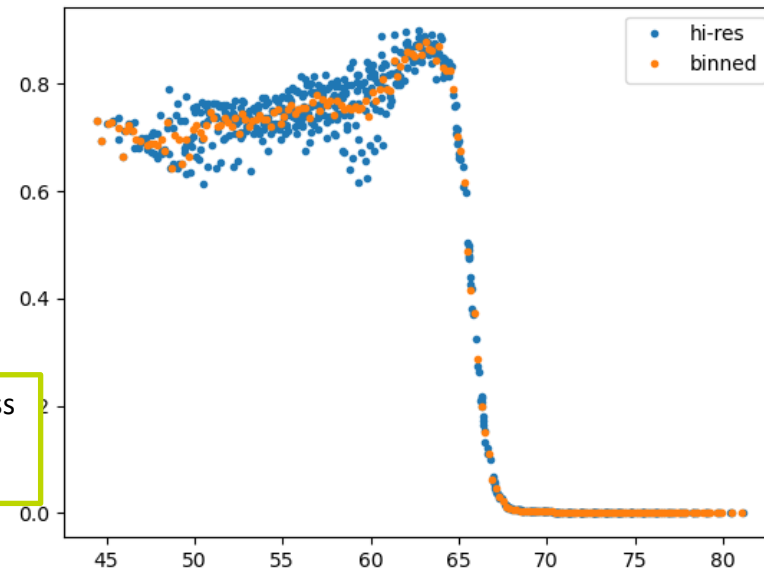


PSF Core calibration based upon adjusting the standard straight edge technique (ISO 12233 ) to the curved edge of the lunar disk. Others have tried this before: [Caron and Rollins, 2020](#).

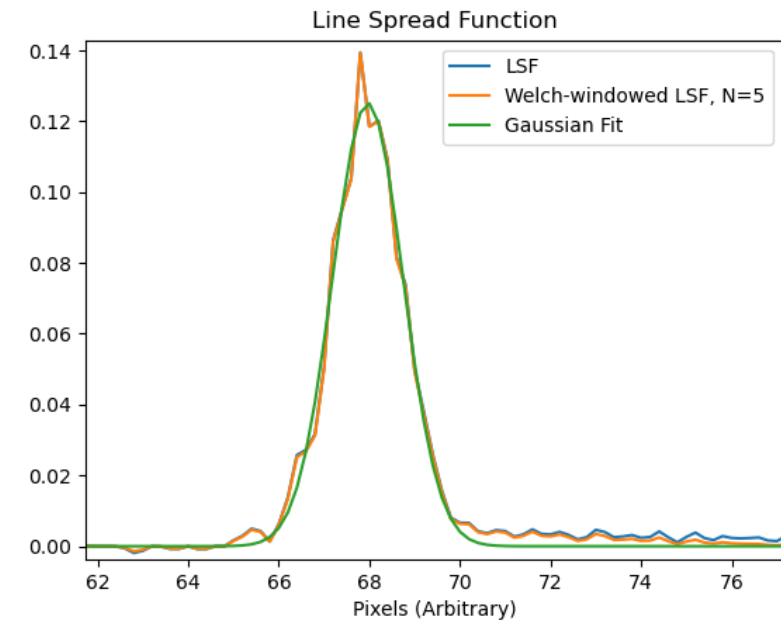
1. Image moon on detector. Select various slices around the edge of the moon



2. For each slice generate an Edge Spread Function (ESF) as a function of radius. This allows super-sampling.

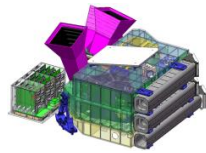


3. Differentiate the ESF to get the Line Spread Function (PSF) and fit a Gaussian curve.



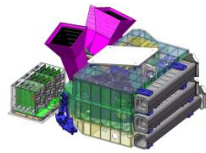
We currently do not flatten the lunar disk using external databases. We can achieve acceptable results as long as we are selective about the slices used.

# Wavelength Registration: UV



- The ALTIUS UV channel consists of 4 stacked Fabry-Perot interferometers.
- Each FPI can set its air-gap to any value between ~400 nm and 1800 nm.
- Different coatings on the FPI units provide the required spectral selection.
- At any wavelength, only two FPI units are spectrally active.

# Wavelength Registration: UV



- The ALTIUS UV channel consists of 4 stacked Fabry-Perot interferometers.
- Each FPI can set its air-gap to any value between ~400 nm and 1800 nm.
- Different coatings on the FPI units provide the required spectral selection.
- At any wavelength, only two FPI units are spectrally active.

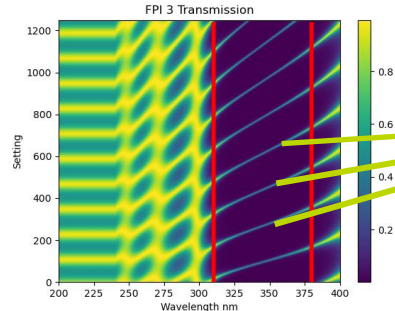
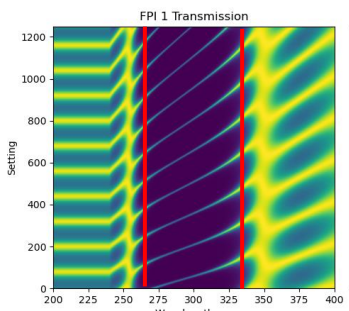
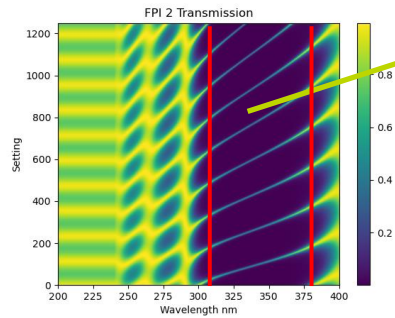
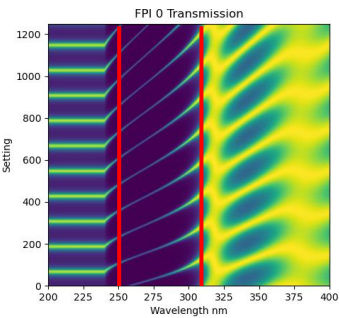
## FPI Transmission

Active below 310 nm

Active above 310 nm

Spectrally active region is between the red lines, where Finesse is high.

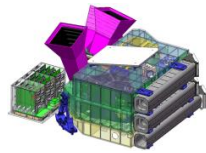
Airgap 400-1800 nm



Spectral Orders ~3 -12

Wavelength 200-400 nm

# Wavelength Registration: UV

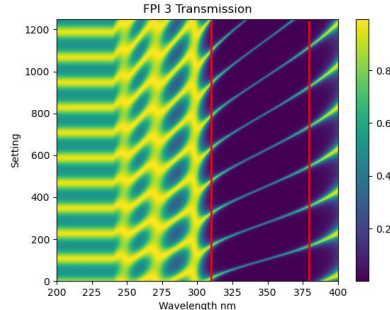
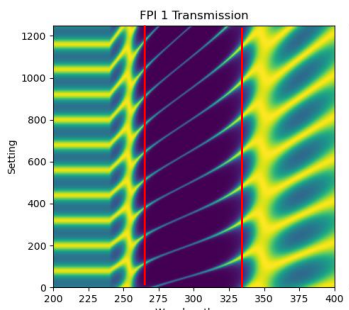
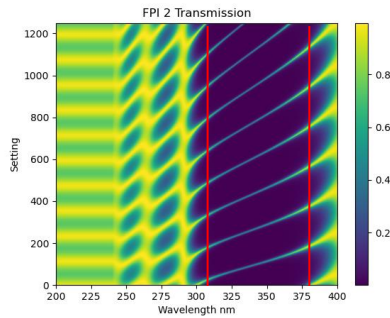
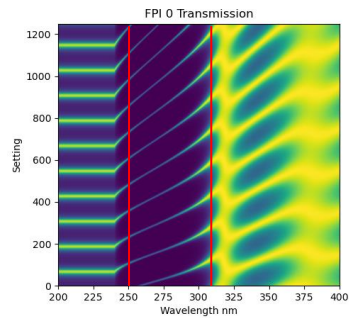


- The ALTIUS UV channel consists of 4 stacked Fabry-Perot interferometers.
- Each FPI can set its air-gap to any value between ~400 nm and 1800 nm.
- Different coatings on the FPI units provide the required spectral selection.
- At any wavelength, only two FPI units are spectrally active.

## FPI Transmission

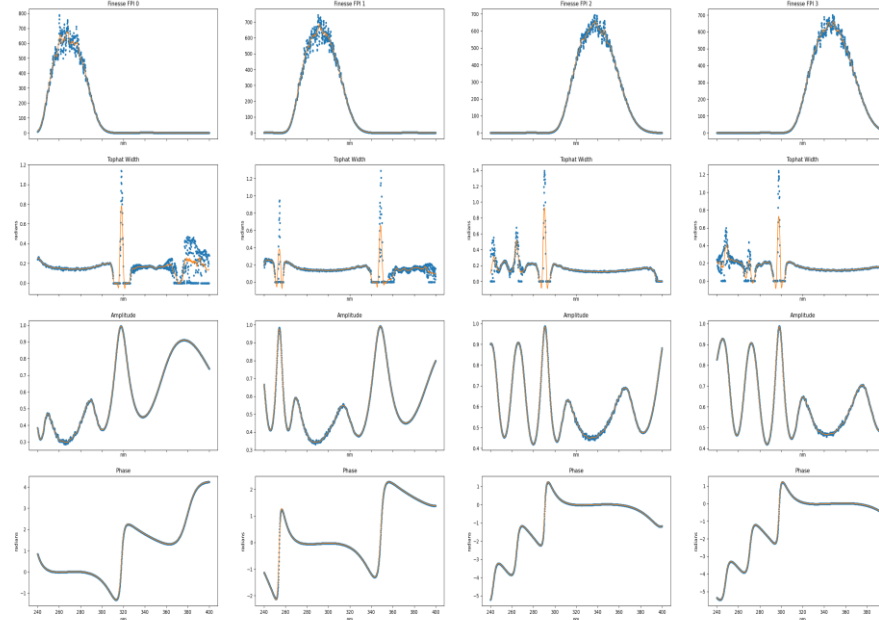
Active below 310 nm

Active above 310 nm



Wavelength 240-360 nm

## FPI: 4 Variable Parameterization



Wavelength 240-400 nm

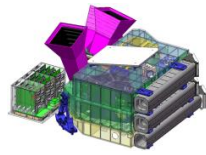
1. Finesse

2. Width

3. Amplitude

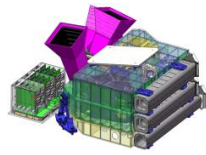
4. Phase

# Wavelength Registration: UV

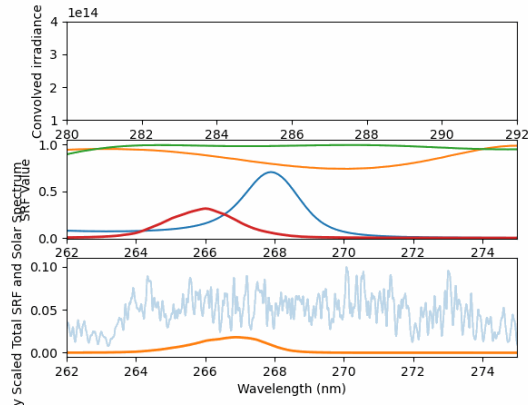


Wavelength registration is determined by calibrating the air-gaps of the FPI units. Only two FPI units are spectrally active at the same time

# Wavelength Registration: UV

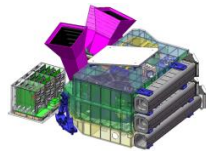


Wavelength registration is determined by calibrating the air-gaps of the FPI units.

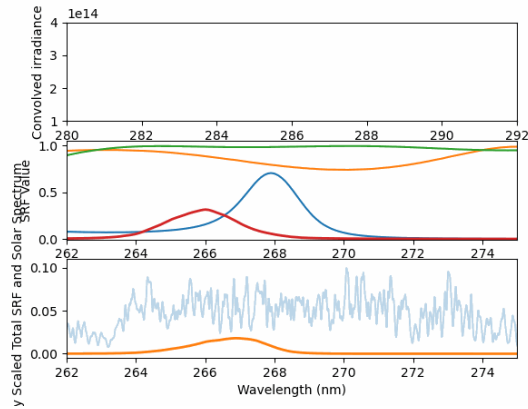


**Step 1:** Measure the relative alignment of the two active FPI units. Hold one FPI constant and scan the other. Choose a flat spectral region.

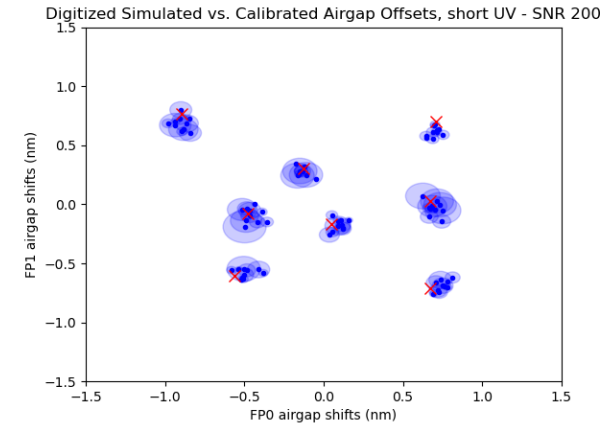
# Wavelength Registration: UV



Wavelength registration is determined by calibrating the air-gaps of the FPI units.

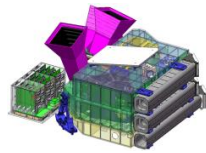


**Step 1:** Measure the relative alignment of the two active FPI units. Hold one FPI constant and scan the other. Choose a flat spectral region.

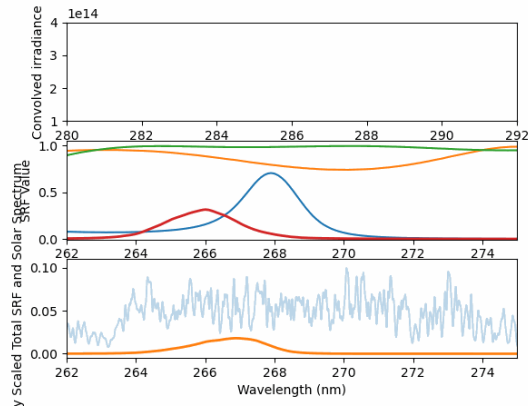




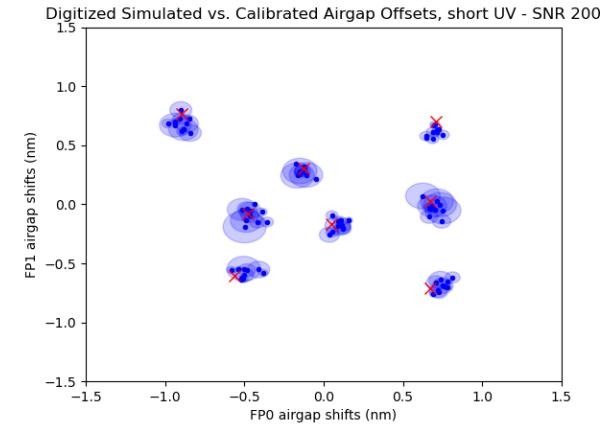
# Wavelength Registration: UV



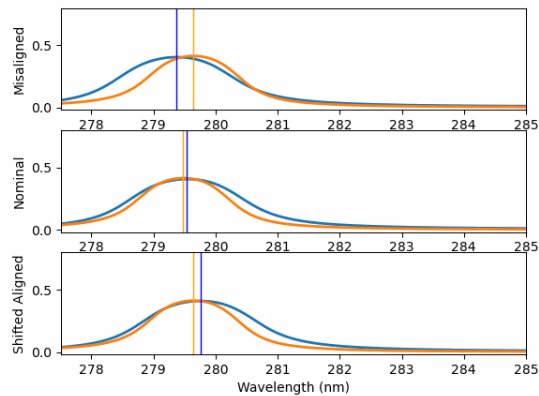
Wavelength registration is determined by calibrating the air-gaps of the FPI units.



**Step 1:** Measure the relative alignment of the two active FPI units. Hold one FPI constant and scan the other. Choose a flat spectral region.

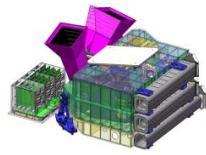


Stage 2 Scan - FP0 offset -0.60 nm, FP1 offset 0.74 nm

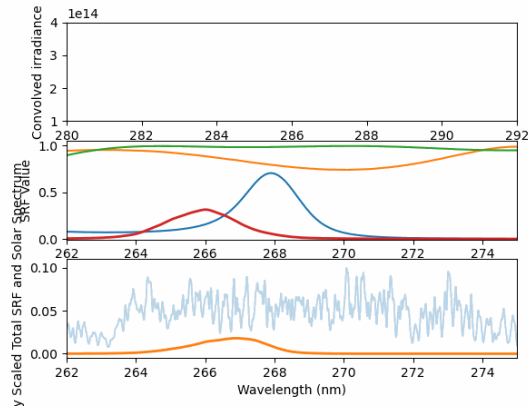


**Step 2:** Scan the two active FPI units across a spectral region. Choose a region with good spectral detail.

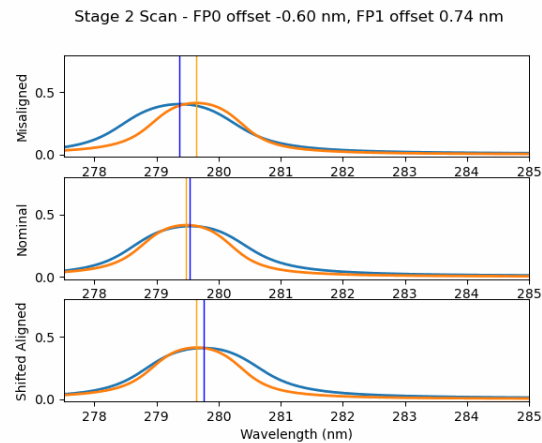
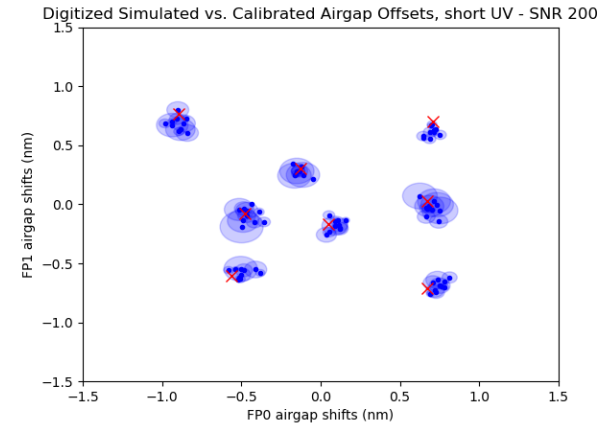
# Wavelength Registration: UV



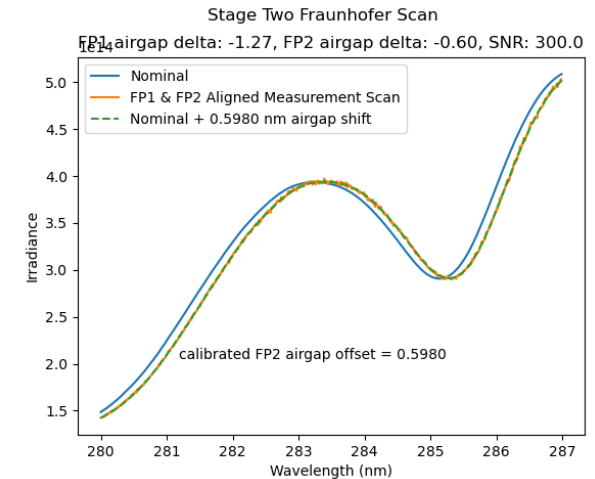
Wavelength registration is determined by calibrating the air-gaps of the FPI units.



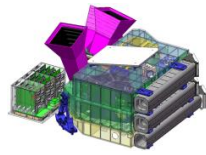
**Step 1:** Measure the relative alignment of the two active FPI units. Hold one FPI constant and scan the other. Choose a flat spectral region.



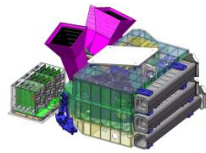
**Step 2:** Scan the two active FPI units across a spectral region. Choose a region with good spectral detail.



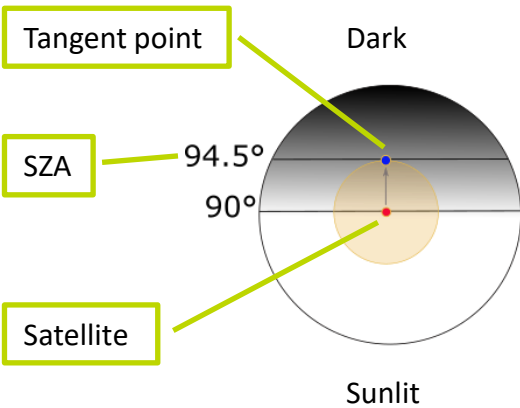
# Polarization

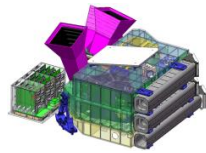


- The NIR and VIS channels have a strong linearly polarized response.
- We can use the atmosphere as a source of known polarization state. We use 60 km tangent altitude when the tangent point is at a solar zenith angle of 94.5 degrees. This geometry suppresses upwelling ground albedo.

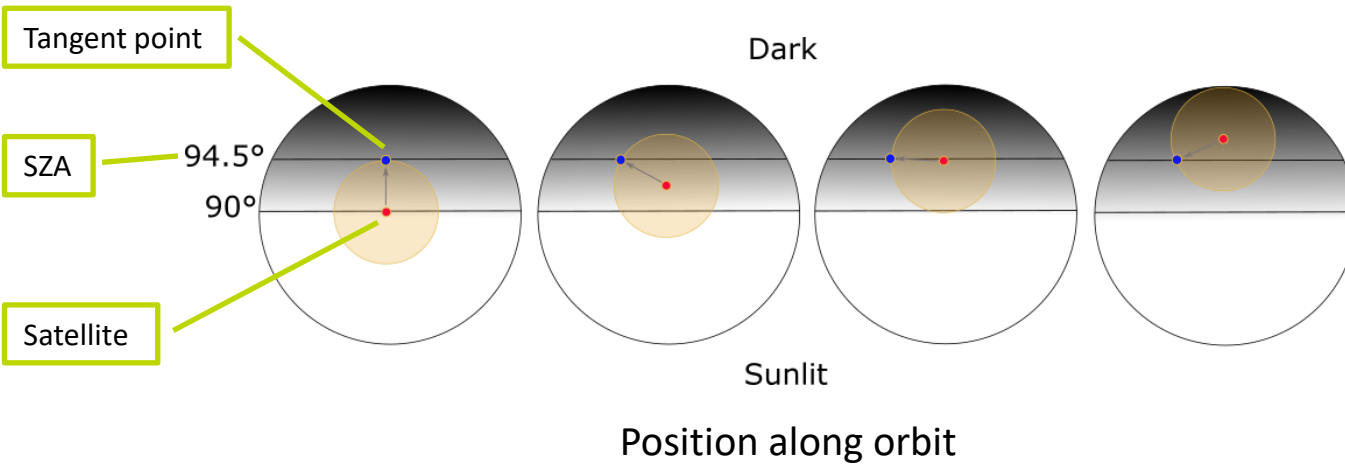


- The NIR and VIS channels have a strong linearly polarized response.
- We can use the atmosphere as a source of known polarization state. We use 60 km tangent altitude when the tangent point is at a solar zenith angle of 94.5 degrees. This geometry suppresses upwelling ground albedo.
- As the satellite moves from dayside to darkness (or vice-versa) it rotates to stare at the tangent point at 94.5 degrees.

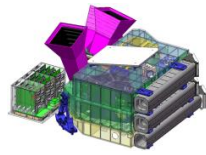




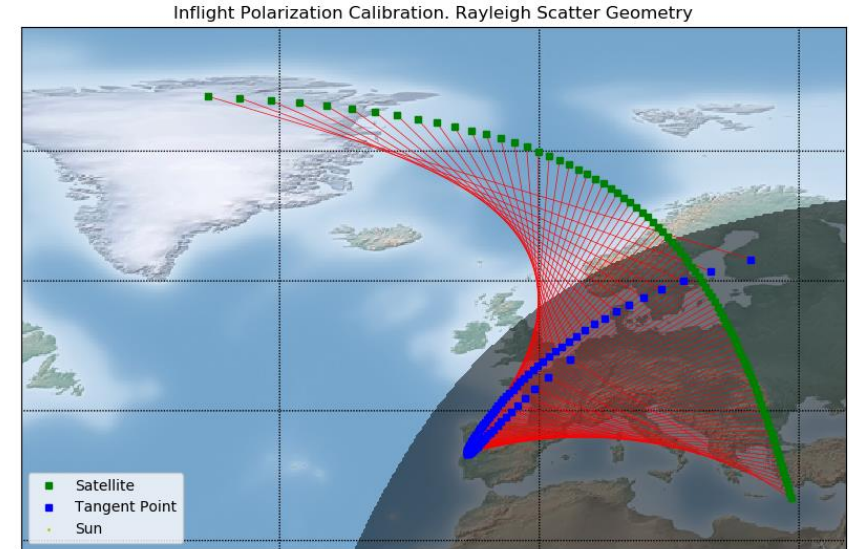
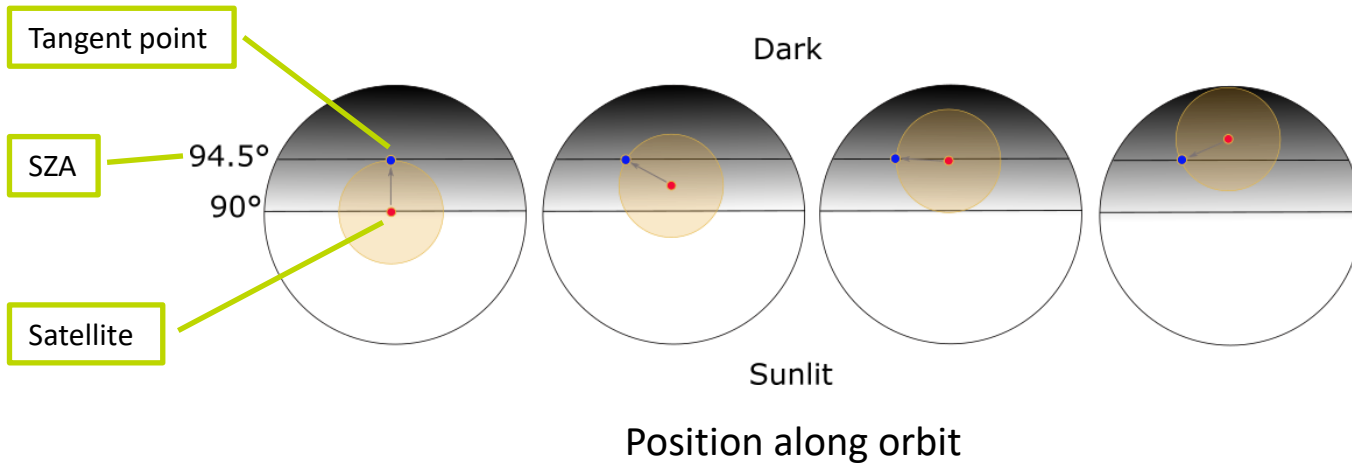
- The NIR and VIS channels have a strong linearly polarized response.
- We can use the atmosphere as a source of known polarization state. We use 60 km tangent altitude when the tangent point is at a solar zenith angle of 94.5 degrees. This geometry suppresses upwelling ground albedo.
- As the satellite moves from dayside to darkness (or vice-versa) it rotates to stare at the tangent point at 94.5 degrees.



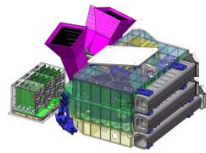
# Polarization



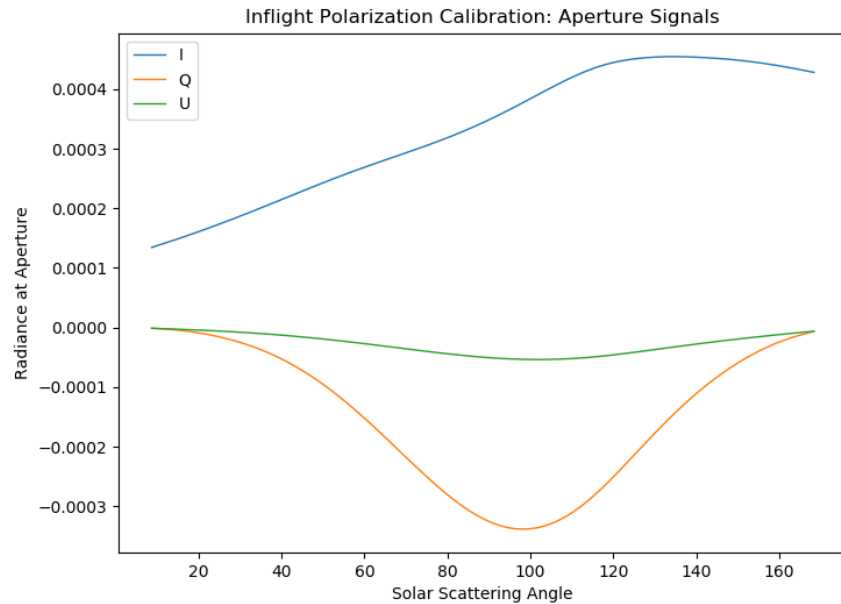
- The NIR and VIS channels have a strong linearly polarized response.
- We can use the atmosphere as a source of known polarization state. We use 60 km tangent altitude when the tangent point is at a solar zenith angle of 94.5 degrees. This geometry suppresses upwelling ground albedo.
- As the satellite moves from dayside to darkness (or vice-versa) it rotates to stare at the tangent point at 94.5 degrees.



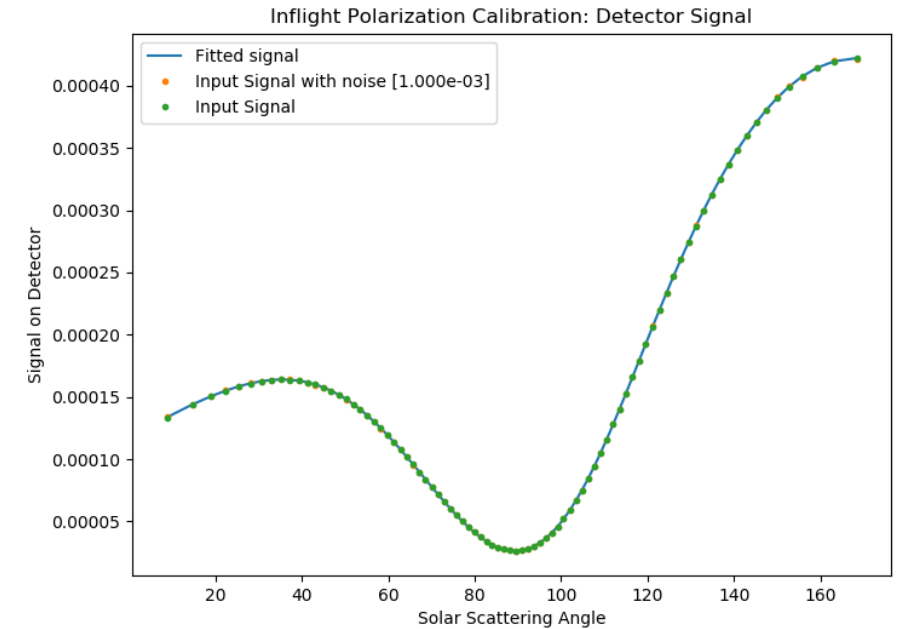
# Polarization



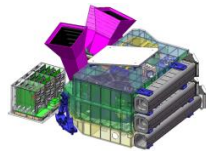
Analysis of the measured signals coupled with a single scatter radiative transfer model allows estimation of  $G_{11}$ ,  $G_{12}$  and  $G_{13}$  for the first row of the polarization (Mueller?) matrix



$$\mathbf{G} = \begin{pmatrix} 1.0 & 0.99 & 0.01 & 0.0 \\ 0.99 & 0.99 & 0.01 & 0.0 \\ 0.01 & 0.001 & 0.001 & 0.0 \\ 0.001 & 0.001 & 0.001 & 0.0 \end{pmatrix}$$



# In-flight calibration Summary



The ALTIUS in-flight calibration is progressing well. We have implemented in-flight calibration techniques that meet instrument requirements. They have been applied to the current instrument design and work quite well.

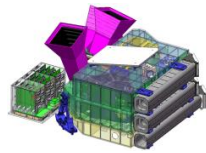
Work is ongoing and we are currently completing absolute calibration.

In-flight measurement of the instrument SRF using natural sources is a challenge that we have not yet conquered.

All analysis to date has been based upon instrument simulation. We expect the techniques to be refined in the coming days as true instrument performance is measured during ground calibration.



# In-flight calibration Summary



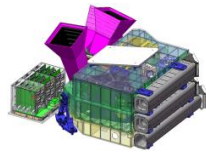
The ALTIUS in-flight calibration is progressing well. We have implemented in-flight calibration techniques that meet instrument requirements. They have been applied to the current instrument design and work quite well.

Work is ongoing and we are currently completing absolute calibration.

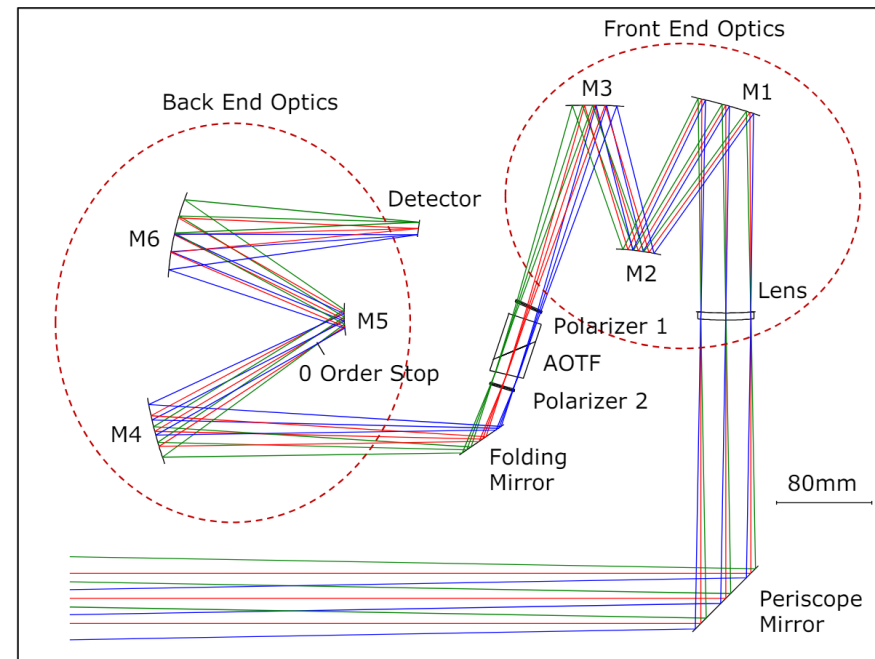
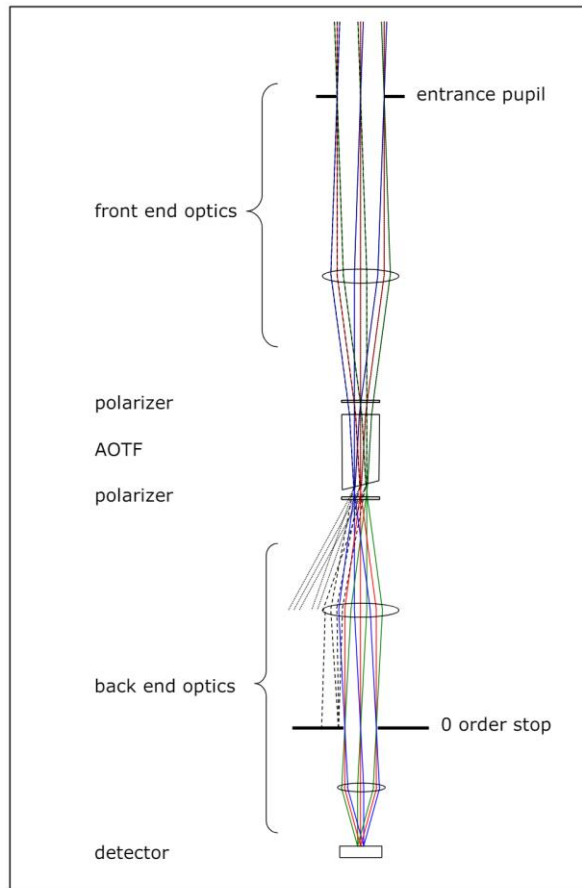
In-flight measurement of the instrument SRF using natural sources is a challenge that we have not yet conquered.

All analysis to date has been based upon instrument simulation. We expect the techniques to be refined in the coming days as true instrument performance is measured during ground calibration.

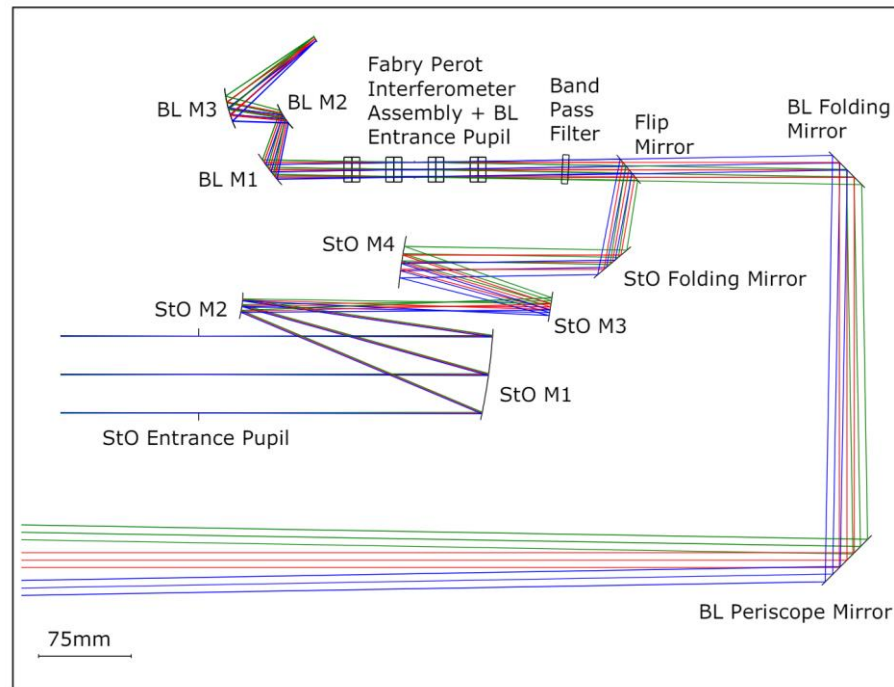
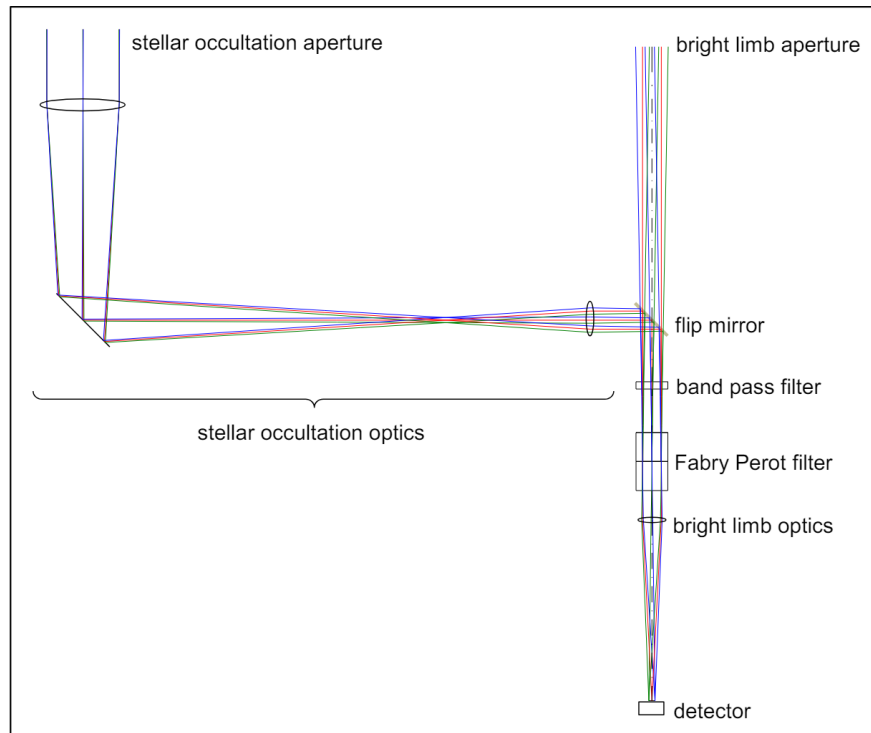
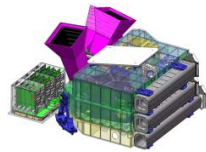
# Thank you



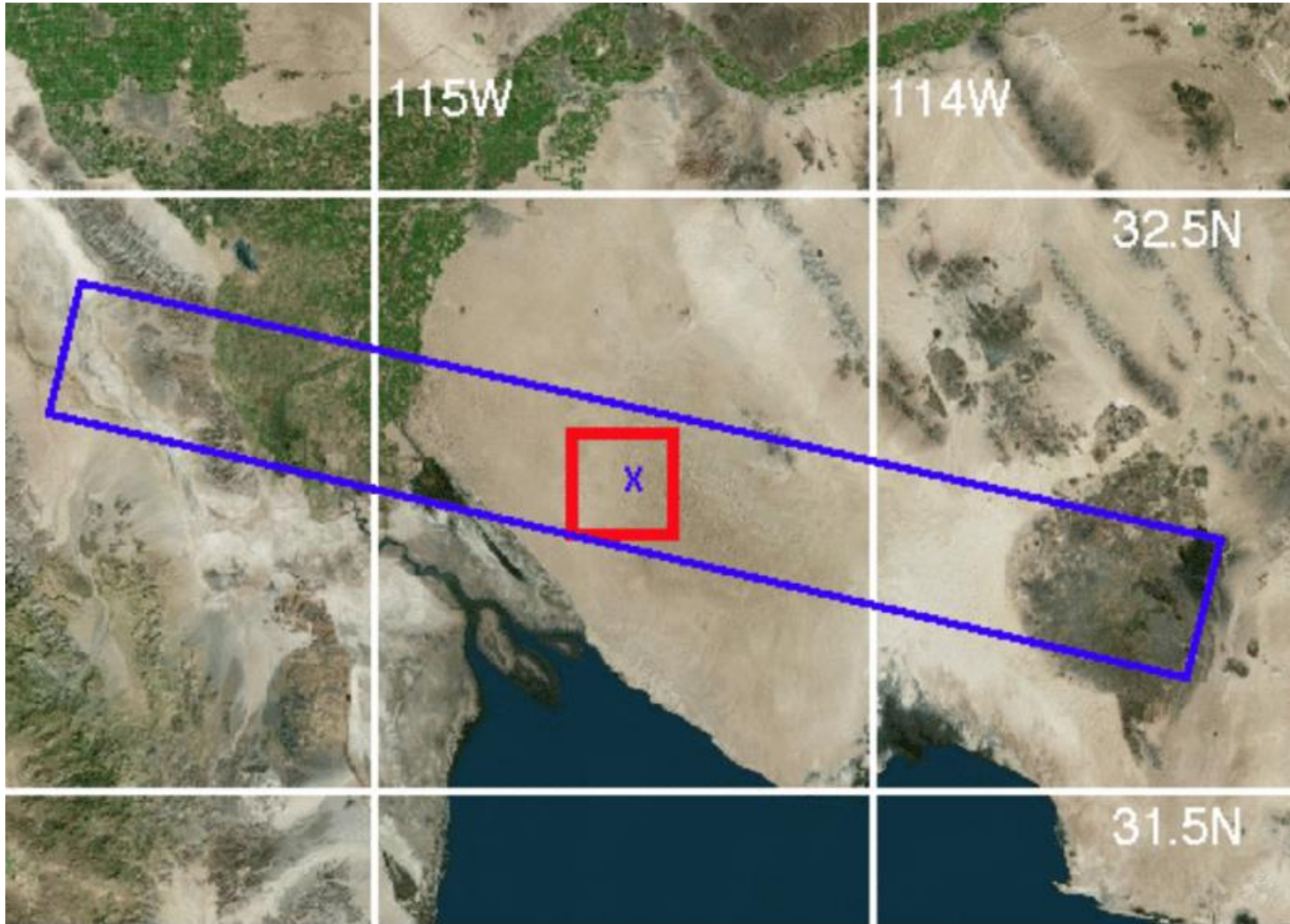
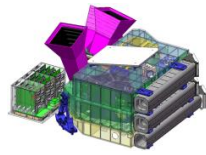
VIS and NIR channels use a telecentric design:



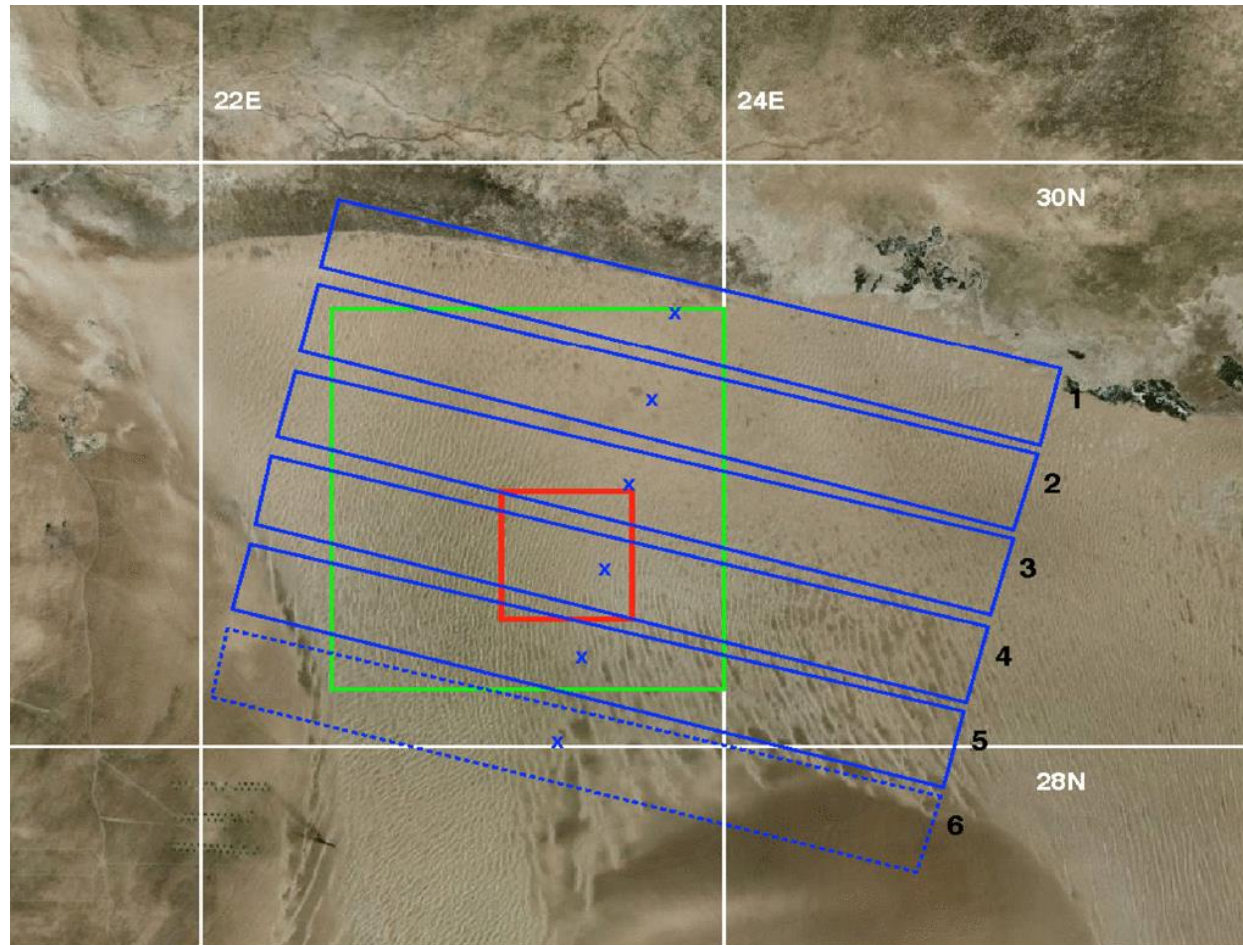
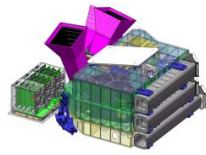
# UV Optics

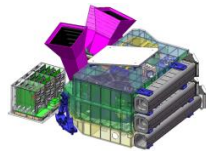


# Libyan Desert



# Libyan Desert

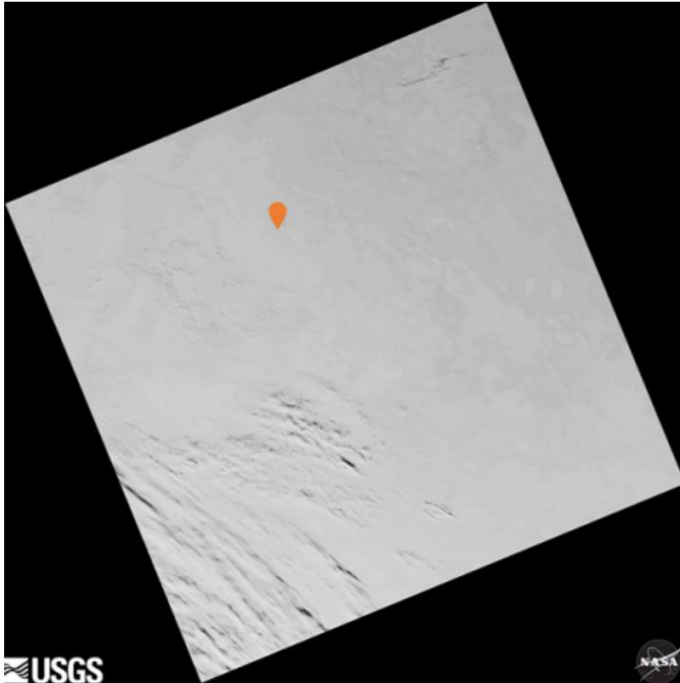




EROS Cal/Val Center of Excellence (ECCOE)

Test Sites Catalog

Dome C

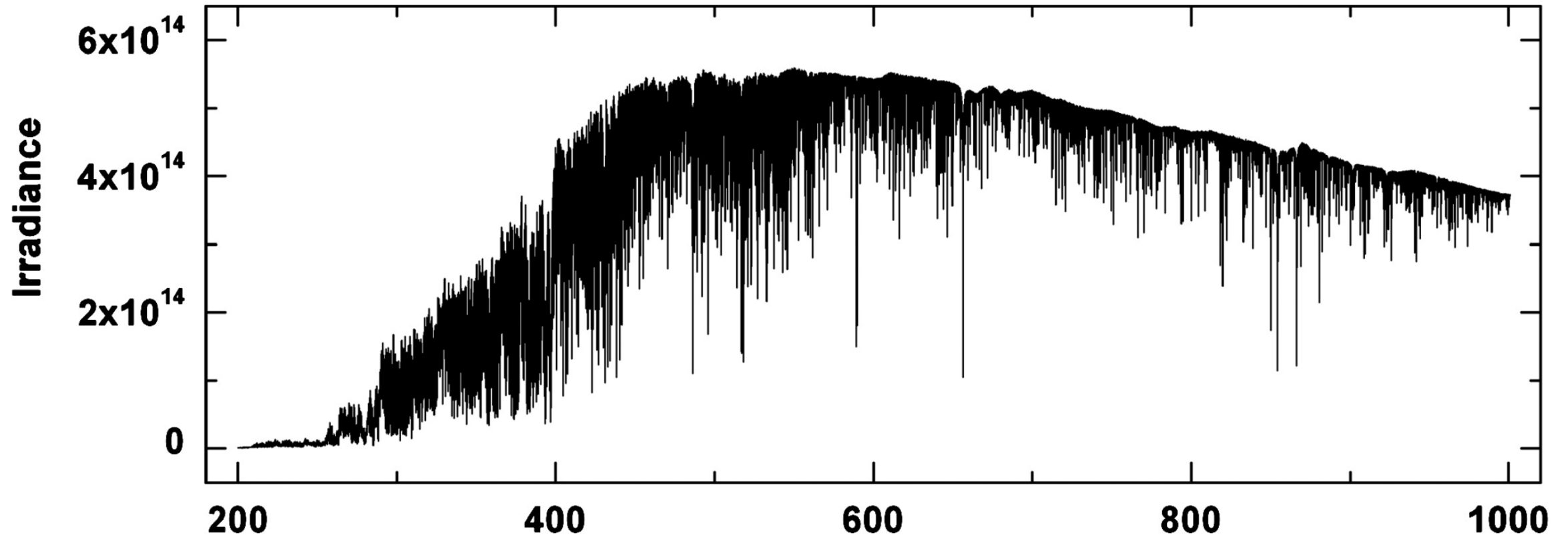
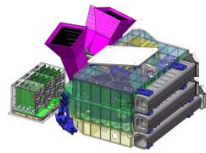


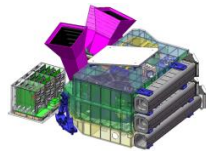
Landsat 8 LandsatLook Image Path 88 Row 13 Acquired 13 Feb 2020 with ROI indicated



Google Earth Image centered on Dome C ROI

<https://calval.cr.usgs.gov/apps/dome-c>





Lunar Irradiance: Cindy Young, Greg Holsclaw and Martin Snow

